FRAZER-NASH CONSULTANCY
A KBR COMPANY

Research into Suitability of Solder and Brazing Alloys for Use in Low Pressure Hydrogen Gas Installations

Final Report

August 2024

021105

56922R Issue: 1

Prepared for: Department for Energy Security and Net Zero

SYSTEMS ● ENGINEERING ● TECHNOLOGY

Originating Office: FRAZER-NASH CONSULTANCY LIMITED
Hill Park South, KBR Campus, Springfield Drive, Leatherhead, Surrey, KT22 7LH
Tel: +44 (0)1306 885050

Executive Summary

The Department for Energy Security and Net Zero (DESNZ) is responsible for supporting the UK transition to a hydrogen economy. The use of hydrogen is an important, possibly essential, part of the UK Government's strategy to achieve the legally binding decarbonisation commitment by 2050. To support this transition, technical standards, competence frameworks, and training specifications for installers are required for domestic and non-domestic installations. These standards will define the required criteria to safely repurpose existing natural gas equipment for hydrogen, to design and install new hydrogen-safe pipework and appliances, and to train a workforce of competent hydrogen gas installers. Contracted by DESNZ, Frazer-Nash Consultancy have assessed the compatibility of hydrogen with solder and brazing alloys used to form the joints in copper pipework, this report summarises all project activity.

The suitability of solder and brazing alloys for use with hydrogen was assessed through tensile testing of copper pipework containing soldered and brazed joints at extension rates of 1.00, 0.10, and 0.01 mm/min; corresponding to average strain rates of 1.4×10^{-4}, 1.4×10^{-5}, and 1.5×10^{-6} s^{-1} respectively. The ultimate tensile stress and strain to failure of the samples were used as the basis of the analysis. Soldered joints were tested using four different combinations of flux and solder: a leaded solder, a lead-free solder, a self-cleaning flux, and a tinned flux. Brazed joints were made using a copper phosphorous braze filler. The tensile tests were conducted under different hydrogen environments of 1 bar gaseous hydrogen, and hydrogen charging (where specimens were chemically pre-charged with hydrogen as well as filled with 1 bar gaseous hydrogen). These results were compared to baseline tensile test results conducted in air. Testing was conducted at room temperature and at an elevated temperature of 50 °C.

The flux and solder combination used to make the joint, in either the coupler or swaged joint geometry, appears to make no significant impact on the joint mechanical capacity. The loading behaviour of the sample under tension was found to be dominated by the base copper piping. Testing in gaseous hydrogen, achieved through filling the samples with 1 bar hydrogen, has no clear impact on joint mechanical capacity. Absorbed hydrogen, achieved through hydrogen charging, appears to have a measurable impact, with a small reduction in ultimate tensile stress observed over most hydrogen charging series relative to their respective baseline series. Following hydrogen charging, the Alloy 12 soldered samples generally demonstrated a decrease in mean strain at failure (with an increased variability) relative to baseline testing, whereas the Alloy 23 soldered samples mostly showed an increase in strain at failure. This is not observed for the pipe or brazed samples. It is believed the hydrogen conditions as tested are more extreme than would be seen in service; testing an absorbed level of hydrogen – through charging – higher than the sample would reach over its 50-year lifetime at 250 mbar service.

The experimental work and statistical analysis provide evidence to support the use of solder and brazing alloys in low pressure hydrogen gas installations. The decrease in joint mechanical capacity as measured by a reduction in ultimate tensile strength and strain at failure is small. In service, the pipes and associated joints will not be loaded to the same extent they were in testing. Other factors such as joint quality and temperature, were observed to have a more significant reduction in joint mechanical capacity. Further work, if deemed necessary could focus on further slow strain rate testing, fatigue testing, and quantifying the hydrogen uptake of the charging technique used.

1 Introduction

1.1 Context

The transition to a hydrogen economy requires infrastructure and associated standards for the performance of this infrastructure, its installation, and its ongoing monitoring and inspection, and the health and safety of installers, users, and the public is of paramount importance. The Department for Energy Security and Net Zero (DESNZ) is responsible for supporting the UK transition to a hydrogen economy and is undertaking a range of work to ensure the fitness for purpose of both the infrastructure supporting the economy and the underpinning standards. Hydrogen can be used in several contexts, one of which is domestic and commercial heating. This raises the possibility of using the existing natural gas network but relies on the network being able to transport hydrogen safely. The DESNZ Hydrogen Skills and Standards for Heat (HSS4H) programme is working towards the development of technical standards for domestic and non-domestic hydrogen gas installations, and on associated competence frameworks and training specifications for installers. These will enable re-purposing of the existing natural gas system to be used with 100% hydrogen downstream of the Emergency Control Valve (ECV). The compatibility of hydrogen and many materials has already been assessed either as part of the DESNZ HSS4H programme or other relevant research streams. One feature present in domestic and non-domestic gas installations yet to be assessed is jointed copper pipework. Jointed copper pipework has previously been assessed by literature review, this research by the Health and Safety Executive (HSE) is reported in IGEM/H/1 [1]. Jointed copper pipework has not yet been experimentally assessed.

DESNZ have contracted Frazer-Nash Consultancy (Frazer-Nash) to undertake the project “Research into Suitability of Solder and Brazing Alloys for Use in Low Pressure Hydrogen Gas Installations”. The purpose of this project is to assess the impact of gaseous hydrogen on jointed copper pipe work, for example, the copper piping used to connect the gas supply to a boiler in a domestic household. Specifically, the question relates to the use of existing domestic and commercial natural gas pipeline infrastructure to deliver hydrogen safely, without remediation. To date, consideration has been on the impact of hydrogen gas on the copper itself, whereas this project will focus on the impact to solder and brazing materials used in joints. Through the DESNZ HSS4H programme, a series of hydrogen standards and training specifications will be developed. The evidence generated within this project will support the development of these technical standards, for domestic and non-domestic hydrogen gas installations, and on associated competence and training requirements for installers [2].

1.2 Aims and Objectives

The purpose of this report is to provide a comprehensive review of all project activities and summarise the results of the work undertaken by Frazer-Nash. This will include:

- Materials testing scope.
- Description of experimental and operational procedures.
- Testing programme.
- Results and analysis.
- Summary of results and concluding remarks.

1.3 Outline

The project was divided into three stages:

- Stage 1: Detailed Test Plan.
- Stage 2: Materials Testing Programme.

- Stage 3: Interpretation of Evidence for Standards

This document will detail how each of these three project stages has been achieved and provide justification to the approach taken. This document is the last of four project deliverables, where previous deliverables include:

- Deliverable 1: Project Inception Meeting.
- Deliverable 2: Detailed Test Plan - 021105-55582R [3].
- Deliverable 3: Interim Report and Presentation – 021105-55861R [4].

2 Materials

2.1 Review of Original Material Scope

Table 2.1 details the list of solder and brazing alloys, and associated materials to be tested, as specified by the original ITT [2].

Table 2.1 – Materials grades and their relevant standards to be used in the the material testing programme, specified in original ITT (adapted from [2]).

Function	Material	Standard
Parent material (pipework)	Copper alloy	BS EN 1057 grades (after 1996) BS 2871 Part 1 (before 1996) BS EN 1254-1 (fittings)
Flux		ASTM B813 – One self-cleaning type ASTM B813 – One tinned type Both for soldered joints
Filler metals	Solder and brazing alloys	BS EN 29453 alloy 11 (solders) BS EN 29453 alloy 12 (solders) BS EN 29453 alloy 13 (solders) BS EN 1044 (braze filler) Brazed Joint to be made to BS EN 14324

Whilst developing the original test plan in Phase 1 of the project, it was identified that the composition specified by BS EN 29453 for alloys 11, 12, and 13 is similar, with alloys 11, 12, and 13 having tin to lead ratios of 63/37, 60/40, and 50/50, respectively. Alloy 13 may have been used in the past but proved difficult to obtain, with the only distributor requiring a substantial minimum order quantity. On this basis, it was proposed to focus on alloy 12 as the primary lead-based solder for consideration with the 60/40 tin to lead ratio, being the standard leaded solder of choice for most plumbing installations. To replace alloys 11 and 13, it was proposed that alloy 23 should be tested; alloy 23 is a widely used lead-free solder to BS EN 29453 with composition 99/1 tin to copper, commonly referred to as 99C.

2.2 Materials Tested

The materials tested, and their relevant standards are detailed in Table 2.2. All materials were procured by Frazer-Nash and the supplier or manufacturer either stated, or provided certification stating, the compliance of the product to the relevant standard. In order to check compliance, the composition of the solders was analysed using energy dispersive X-ray spectroscopy (SEM EDS); and whilst not definitive, the results are consistent with the compositions expected.

Table 2.2 – Tested materials and their relevant standards used in the the testing programme.

Function	Material	Standard
Parent material (pipework)	15 mm Copper Tube	BS EN 1057 Table X
	15 mm Copper Tube	BS 2871 Part 1
	15 mm F x F Copper Straight Coupling	BS EN 1254-1
Flux	La-Co Soldering Flux	ASTM B813 – Self Cleaning (SC)
	Oatey H20 95 Tinning Flux	ASTM B813 – Tinned (T)
Filler metals	60/40 Leaded Solder	BS EN 29453 Alloy 12
	99C Lead-Free Solder	BS EN 29453 Alloy 23
	STÖRNCH Brazing Rods	BS EN 1044 CP 203 (braze filler)

2.3 Specimens

All samples were 200 mm in length. For jointed samples, the joint was located approximately halfway along the sample length. All sample types as-prepared are shown in Figure 2.1. All soldered samples were prepared by Fareham Plumbing and Heating Ltd by qualified plumbers according to training and industry best practice. Brazed samples were made by EMS Ltd a HVAC specialist in accordance with BS EN 14324.

Figure 2.1 – Different specimen types, photographed as-prepared.

3 Technical Approach

3.1 Test and Specimen Arrangement

Tensile tests were undertaken using an Instron 5500R Universal Testing Machine (UTM) and controlled using Bluehill Universal (version 4.43), Instron's proprietary software. Figure 3.1 shows the UTM set-up, as-tested, with various ancillary equipment labelled. For consistency, the same test frame, attachments and grip assemblies were used for all tests. All attachments were suitable for testing at loads up to and including 100 kN. A Pickstone Ovens Thermal Test Chamber was used for testing at elevated temperature, which can be seen behind the test frame in Figure 3.1.

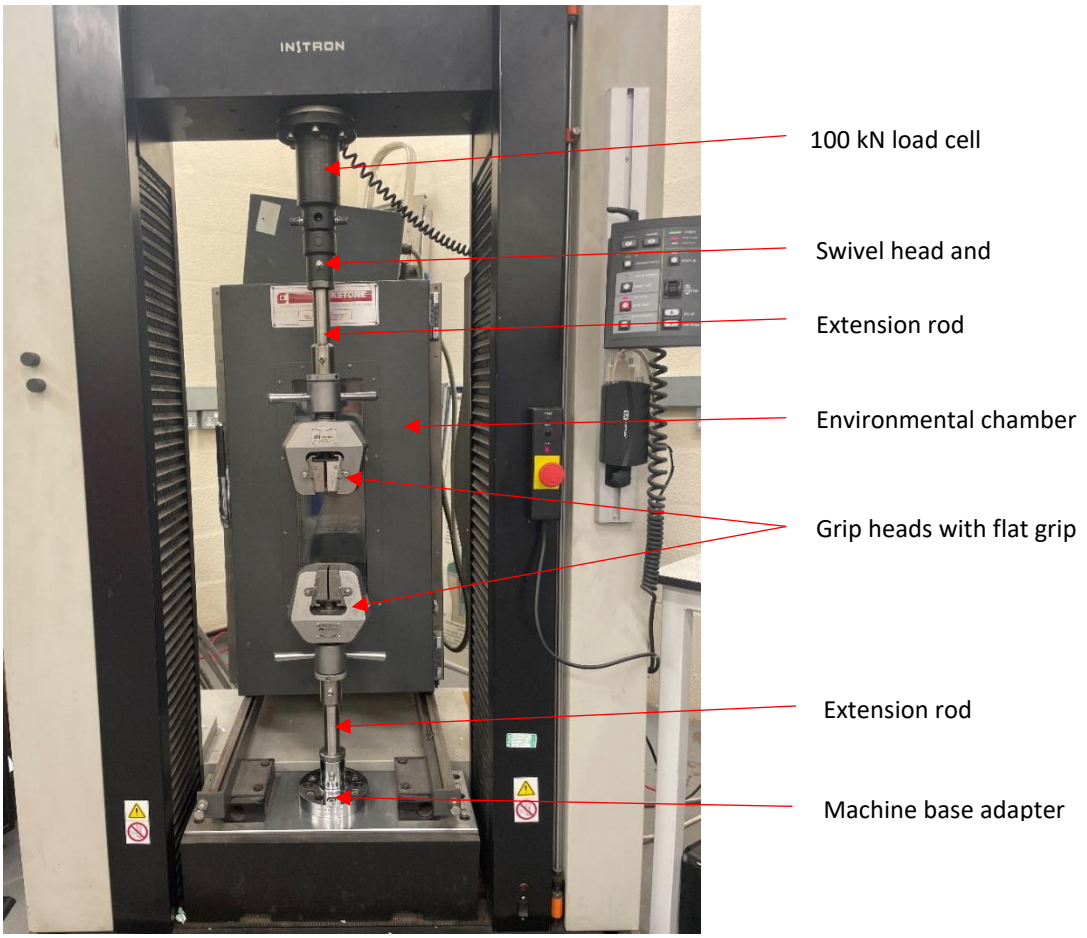

Figure 3.1 – Instron 5500R test frame with load cell, attachments, and grip assemblies as tested.

As labelled in Figure 3.1, a set of Instron flat grips were used to grip the specimens at each end. To facilitate this, the samples were flattened prior to testing using a Klauke EK 135 handheld hydraulic crimping tool fitted with a custom set of flat plates, which were manufactured for this device to crimp the ends flat with a force of 135 kN. A small amount of cyanoacrylate adhesive[1] was spread inside the pipe rim prior to crimping which allowed for a gas tight seal to be achieved, with 1 bar of hydrogen. This flattened surface provided a dependable gripping surface for consistent tensile testing with no slippage. A flattened pipe sample is shown in Figure 3.2A.

[1] As the cyanoacrylate adhesive cures, small amounts of formaldehyde, water vapour, and potential other minor organic compounds may be released as biproduct [14]. The release of these compounds is not anticipated to impact hydrogen absorption and resulting effects.

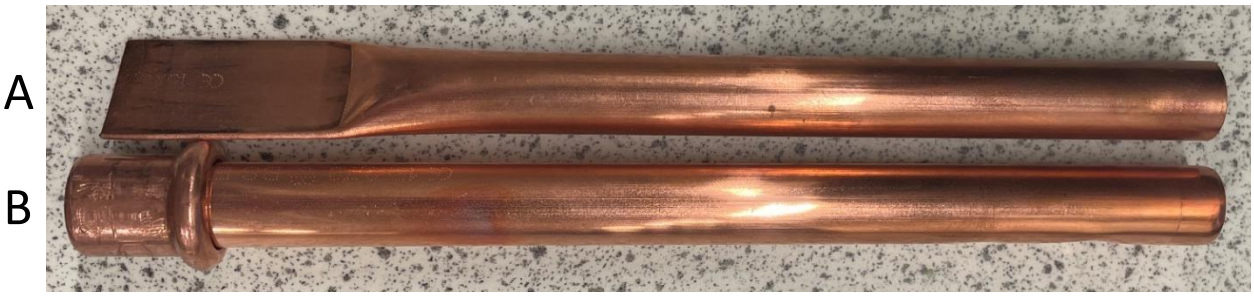

Figure 3.2 – A – Flattened, crimped pipe sample, B, round pipe sample, with gas a certified end cap.

It was found when the ends were crimped flat with the Klauke EK 135 crimping tool, the crimp line presented a possible point of failure, with approximately 30% of samples crimped in this manner failing at the crimp line. To mitigate this, the samples were double crimped, first using the Klauke EK 135 handheld hydraulic press, and subsequently using a set of flat compression plates on an Instron 5500R UTM with pressing force of 80 kN. The lower force and slight hemispherical edge of the compression plates resulted in a less defined crimp line, resulting in only ~5% of samples crimped in this manner failing in the gripped region.

3.2 Round Specimen Grips

Early in the project, it was established that it would not be possible to procure or obtain round specimen grips in a timely, cost effective manner. Since a commercially available solution was not possible, a considerable amount of time was spent designing a set of round specimen grips. These grips were designed to grip the pipe circumferentially whilst accommodating a gas certified push fit end cap, which can be seen in Figure 3.2 B. This would preclude the need to flatten the pipes, as well as permit testing of the pipes in their true in field geometry. The round grips can be seen in Figure 3.3. These grips are classed as chuck-style wedge grips, where a geared mechanism controls a set of four jaws which clamp onto the pipe with radial symmetry. This chuck has been adapted to the Instron pin system so it can be mounted onto the UTM for tensile testing.

The gripping force of the jaws when tightened via the chuck tightening key was insufficient to grip the samples for tensile testing, with the specimens slipping at the grip points at prior to failure. This motivated the design of the collar in Figure 3.3, which uses four bolts to tighten onto the jaws, which provides sufficient gripping force to grip the samples for tensile testing without slip occurring. In addition, to the grip assembly shown in Figure 3.3, 13 mm steel plugs were placed in each end of the copper pipe which filled the void in the copper pipe from the end cap up to the top of the pin jaws, whilst the plugs prevent the jaws from crushing the pipe.

The custom round specimen grip assembly was successfully used to conduct 38 baseline tests. Unfortunately, the reliability of this assembly was not satisfactory, with approximately 20% of samples failing at the top of the plugs, samples slipping, and ultimately failure of the collar system owing to fatigue in the threads. Considering the time critical nature of this project, the decision was made to complete testing using the more reliable flat grips.

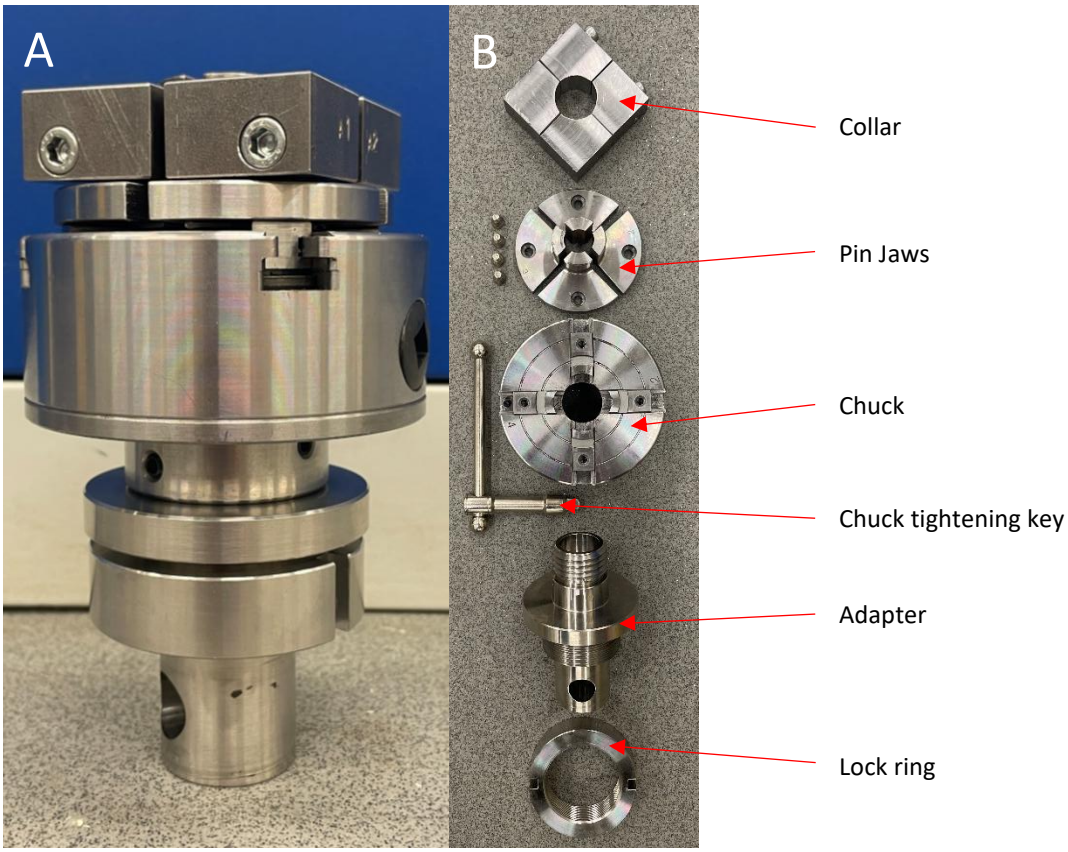

Figure 3.3 – Custom made round jaws and accessories. A, shown as assembled. B, disassembled and labelled.

3.3 Environmental Pretreatment – Immersion Charging

Immersion charging was selected as the pre-charging method (see Annex A1 for the reasoning behind this method selection). Specifically, the samples were immersed in a 20% ammonium thiocyanate (NH_4SCN) aqueous solution at 50 °C for 72 hours. The setup used is shown in Figure 3.4.

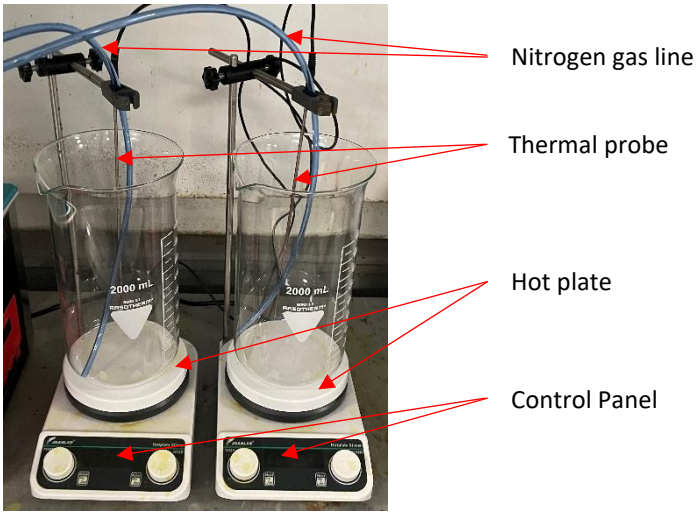

Figure 3.4 – Hydrogen pre-charging setup, situated inside fume hood with key features labelled.

The 20% NH_4SCN solution was prepared by mixing ~1.6 L of ultrapure water with ~400 g of powdered NH_4SCN (≥98% purity). For one hour prior, and throughout the 72-hour charging period, nitrogen gas (99.998% purity) was gently bubbled through the solution at ~0.1 bar to displace oxygen. The purpose of this was to limit oxidation of the sample, as an oxide layer will inhibit hydrogen entry. This initial one-hour period (prior to starting hydrogen charging) also allowed the solution to reach and stabilise at 50 °C. The temperature was measured through the thermal probe positioned in the solution.

While gaseous charging was considered the preferred test environment, as it more representative of in-service conditions, the timeline of this project prevented its use given the number of samples tested. The use of NH_4SCN as a hydrogen charging reagent is common in steel research, and considered an appropriate, valid alternative [5]. It is expected that an absorbed level of hydrogen between 1 and 5 ppm[2] is achieved using this technique (based on the basic calculations in Annex A1), whilst limiting inadvertent corrosion or other chemical attack. This ppm level is most likely more than would be seen in service for copper pipes operating at 250 mbar hydrogen for 50 years. However, it is recognised that these calculations are simplistic, and the data used to estimate hydrogen absorption is for copper, since the data for the solder and brazing material is not available.

To verify NH_4SCN did not cause excessive damage to the sample, trials were run using a 10% and 20% NH_4SCN solution. Figure 3.5 shows the change in absolute mass measured for both trials. For the 10% solution, an increase in mass was observed for all samples which can be attributed to the formation of the white salt-like compound (an example of which is shown in Figure 3.6 for the brazed specimens). This white solid did not form for the 20% solution and no significant mass change was measured for either the lead-free or leaded soldered samples. The mass loss recorded for the brazed sample in 20% NH_4SCN is likely due to dissolution of the oxide layer near the brazed joint, this can be observed in Figure 3.6.

Other observations during experimental testing indicated that the NH_4SCN charging resulted in successful hydrogen absorption. For example, bubbles forming at the joint upon jointed failure indicated gas release. Additionally, throughout charging the samples developed a dark film, the appearance of which resembled copper sulphide, indicating the reaction of NH_4SCN with copper, and the likely formation of hydrogen sulphide; the attack of which will result in the absorption of hydrogen into the sample and formation of copper sulphide on the specimen surface.

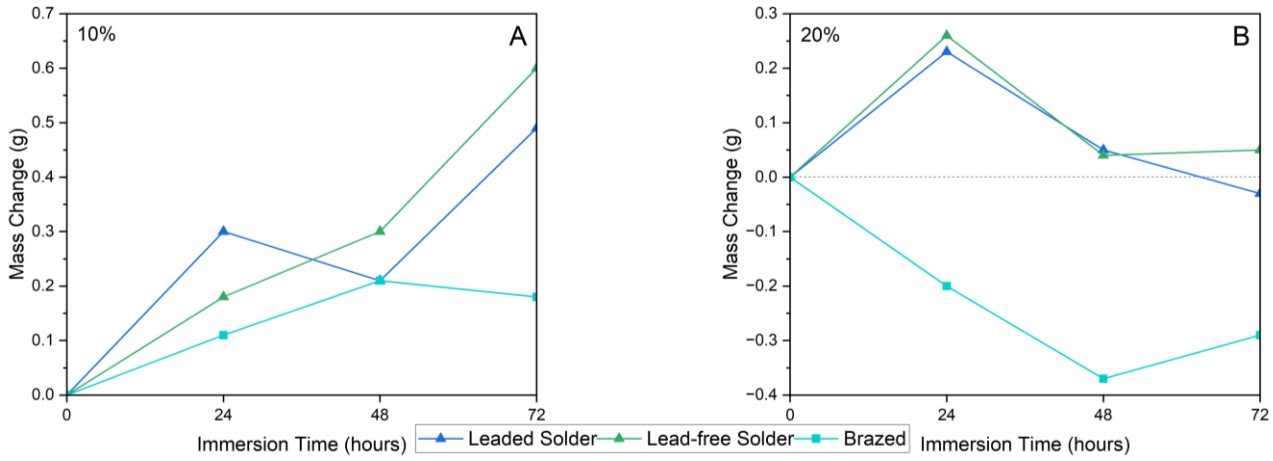

Figure 3.5 – Change in mass for jointed samples in immersion trial. Each point represents one sample, with one sample trailed for each condition. A, 10% ammonium thiocyanate solution. B, 20% ammonium thiocyanate solution.

[2] ppm throughout this report is referring to ppm by volume.

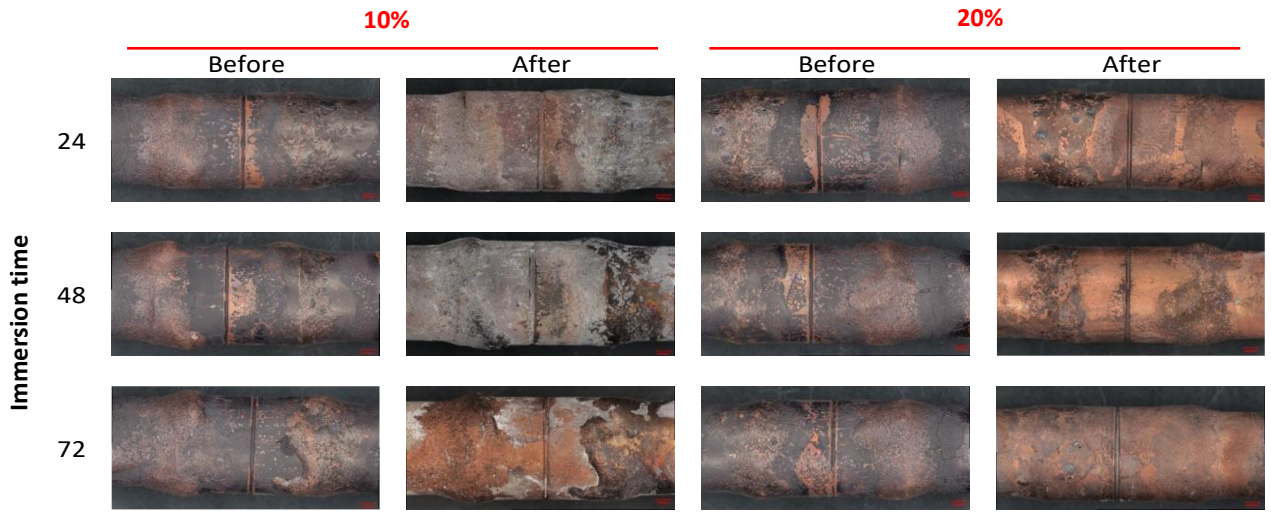

Figure 3.6 – Brazed coupled jointed before and after charging in 10% and 20% ammonium thiocyanate solution.

3.4 Environmental Pretreatment – Gaseous Charging

As discussed in Section 3.1, the samples were flat gripped, which required the ends of the copper pipe to be pressed flat prior to testing. For the baseline testing in air, this flattening was achieved using an Instron 5500R Universal Testing Machine (UTM). For testing in gaseous hydrogen, a filling process was developed. Laboratory grade hydrogen (99.995%) was supplied by an external gas cylinder and line into a fume hood. The flow rate was controlled by a pressure regulator flow meter. Figure 3.7 shows the end of the gas line which was been adapted to a gas certified 15 mm push fitting. All fittings were leak tested by pressurising to ~1 bar[3] of hydrogen, with no leaks detected when using a leak detection fluid.

Figure 3.7 – Gaseous hydrogen filling setup with hydrogen gas line adapted to a 15 mm press fitting used to fill samples. A, push it adapter. B, a pipe in the put fit adapter with the protruding end crimped flat.

To fill and seal the specimens, the Klauke Ek 135 battery powered handheld hydraulic crimping tool was used, described in Section 3.1. Prior to flattening, a small amount of cyanoacrylate adhesive was spread on the inside of the pipe rim at each end, which was found to guarantee a leak free seal. With the regulator set to 1 bar, hydrogen was allowed to flow freely through the pipe to displace air; the protruding pipe end was then crimped flat. To seal the other end of the sample, the pipe was moved to the lip of the connector and the end was crimped flat. Following this, each end was re-crimped by the Instron UTM.

[3] Pressure as used throughout this report is referring to gauge pressure.

4 Testing

4.1 Original Scope

The original test plan from 021105-55582R [3] is shown in Table 4.1 with an assigned code to designate each series of testing and each sample within this series. For instance, for series 2D there are ten samples from 2D1 to 2D10. All tests were to be conducted at an extension rate of 1.00 mm/min.

Table 4.1 – Original mechanical testing plan for the project with assigned codes for each series of testing.

Phase	Joint Type	Parent Material	Flux	Filler	Test Environment	Temperature (°C)	No. of Samples	Series	Total No. of Tests
1 - Baseline Testing	None	BS EN 1057	None	None	Air	-30	10	1A_	140
						23 (RT)	10	1B_	
						50	10	1C_	
	Socket	BS EN 1057 + BS EN 1254-1	SC	12		-30	10	1D_	
						23 (RT)	10	1E_	
						50	10	1F_	
				23		-30	10	1G_	
						23 (RT)	10	1H_	
						50	10	1I_	
			T	12		23 (RT)	10	1J_	
				23		23 (RT)	10	1K_	
			None	CP 203		-30	10	1L_	
						23 (RT)	10	1M_	
						50	10	1N_	
2 - Hydrogen	None	BS EN 1057	None	None	Hydrogen	23 (RT)	10	2A_	120
					Hydrogen + Charging		10	2B_	
	Socket	BS EN 1057 + BS EN 1254-1	SC	12	Hydrogen		10	2C_	
					Hydrogen + Charging		10	2D_	
				23	Hydrogen		10	2E_	
					Hydrogen + Charging		10	2F_	
			T	12	Hydrogen		10	2G_	
					Hydrogen + Charging		10	2H_	
				23	Hydrogen		10	2I_	
					Hydrogen + Charging		10	2J_	
			None	CP 203	Hydrogen		10	2K_	
					Hydrogen + Charging		10	2L_	
3 - Temperature	None	BS EN 1057	None	None	Hydrogen + Charging	-30	10	3A_	80
						50	10	3B_	
	Socket	BS EN 1057 + BS EN 1254-1	SC	12		-30	10	3C_	
						50	10	3D_	
				23		-30	10	3E_	
						50	10	3F_	
			None	CP 203		-30	10	3G_	
						50	10	3H_	
4 - Strain Rate	None	BS 2871 Part 1	None	None	Air	-30	10	4A_	100
						23 (RT)	10	4B_	
						50	10	4C_	
					Hydrogen	23 (RT)	10	4D_	
					Hydrogen + Charging	-30	10	4E_	
						23 (RT)	10	4F_	
						50	10	4G_	
	Socket	BS 2781 Part 1 + BS EN 1254-1	SC	12	Hydrogen + Charging	23 (RT)	10	4H_	
				23			10	4I_	
			None	CP 203			10	4J_	
5 - Practitioner Variability	Socket	BS EN 1057 + BS EN 1254-1	SC	12	Hydrogen + Charging	23 (RT)	50	5A__	100
				23			50	5B__	
6 – Swage	Swaged	BS EN 1057	SC	12	Air	23 (RT)	10	6A_	60
					Hydrogen + Charging		10	6B_	
				23	Air		10	6C_	
					Hydrogen + Charging		10	6D_	
			None	CP 203	Air		10	6E_	
					Hydrogen + Charging		10	6F_	

4.2 Updates to Testing Scope

On delivery of the project interim report and presentation [4], feedback, questions, and the guidance of stakeholders emphasised that slower strain rate testing was of significant value in forming the safety case for the hydrogen compatibility of solder and brazing alloy. As a result, several changes were made to the test plan to include slow strain rate testing at the sacrifice of the low temperature tests.

Slower strain rate testing was included to the test plan at rates of 0.10 mm/min and 0.01 mm/min, corresponding to average strain rates of 1.4×10^{-5} and 1.5×10^{-6} s^{-1} respectively. This testing is additional to the core testing at rates of 1.00 mm/min at an average strain rate of 1.4×10^{-4} s^{-1}. The scope of the slow strain rate testing was limited to three, rather than ten samples for each series of testing. This reduction in number of tests was necessitated by the increased test duration and the time critical nature of this project. The extension rates of 0.10 and 0.01 mm/min were selected for testing, with 0.10 mm/min in line with the guidance of ASTM G142 [6], a standard for gaseous hydrogen slow strain rate testing to evaluate the susceptibility of metals to hydrogen embrittlement. As is standard practise for slow strain rate testing, tests are conducted at strain rates an order of magnitude either side of this, with 0.01 mm/min on this premise being a suitable slowest strain rate.

Testing at -30°C was removed from the original test matrix, again, due to allow the longer duration, slow strain rate testing to be incorporated into the test programme within the defined, critical timescales. The extent of the pervasive effects hydrogen can increase with temperature, during both the entry of hydrogen into the material, and during subsequent movement when thermally activated. As a result, it was determined that testing in hydrogen at -30 °C would provide little added value.

Testing BS 2871 Part 1 copper pipe was also removed from the test matrix. Originally, testing was planned for samples made from 15 mm copper pipe to both BS EN 1057 and BS 2871 Part 1, with BS 2871 Part 1 being the older specification. The pipe specifications overlap, such that the pipe procured for this programme satisfies both BS 2871 Part 1 Table X and BS EN 1057 half-hard requirements. As a result, there was no added value in conducting the phase 4 pipe age testing in the original test plan (Table 4.1).

4.3 Final Test Plan

The final test plan is detailed in Table 4.2. The series code has been reassigned accordingly. Originally (Table 4.1), 600 tests at an extension rate of 1 mm/min were specified. Following the updates to testing scope 180 tests were removed (80 tests at -30 °C and 100 tests for pipe age) and 36 tests at slower extension rates were added bringing the total number of tests to 456. Whilst the total number of tests reduced, the combined duration of the testing increased substantially.

Table 4.2 – The amended and final testing plan for the project with the addition of slow strain rate testing and removal of testing at -30 °C and pipe age testing.

Phase	Joint Type	Parent Material	Flux	Filler	Test Environment	Temperature (°C)	Extension Rate (mm/min)	No. of Samples	Series	Total No. of Tests
1 - Baseline Testing	None	BS EN 1057	None	None	Air	23 (RT)	1.00	10	1A_	100
						50		10	1B_	
	Socket	BS EN 1057 + BS EN 1254-1	SC	12		23 (RT)		10	1C_	
						50		10	1D_	
				23		23 (RT)		10	1E_	
						50		10	1F_	
			T	12		23 (RT)		10	1G_	
				23		23 (RT)		10	1H_	
			None	CP 203		23 (RT)		10	1I_	
						50		10	1J_	
2 - Hydrogen	None	BS EN 1057	None	None	Hydrogen	23 (RT)	1.00	10	2A_	120
					Hydrogen + Charging			10	2B_	
	Socket	BS EN 1057 + BS EN 1254-1	SC	12	Hydrogen			10	2C_	
					Hydrogen + Charging			10	2D_	
				23	Hydrogen			10	2E_	
					Hydrogen + Charging			10	2F_	
			T	12	Hydrogen			10	2G_	
					Hydrogen + Charging			10	2H_	
				23	Hydrogen			10	2I_	
					Hydrogen + Charging			10	2J_	
			None	CP 203	Hydrogen			10	2K_	
					Hydrogen + Charging			10	2L_	
3 - Temperature	None	BS EN 1057	None	None	Hydrogen + Charging	50	1.00	10	3A_	40
	Socket	BS EN 1057 + BS EN 1254-1	SC	12				10	3B_	
				23				10	3C_	
			None	CP 203				10	3D_	
4 - Strain Rate	Socket	BS EN 1057 + BS EN 1254-1	SC	12	Air	23 (RT)	0.10	3	4A_	36
							0.01	3	4B_	
					Hydrogen		0.10	3	4C_	
							0.01	3	4D_	
				23	Hydrogen		0.10	3	4E_	
							0.01	3	4F_	
					Hydrogen + Charging		0.10	3	4G_	
							0.01	3	4H_	
			None	CP 203	Air		0.10	3	4I_	
							0.01	3	4J_	
					Hydrogen		0.10	3	4K_	
							0.01	3	4L_	
5 - Practitioner Variability	Socket	BS EN 1057 + BS EN 1254-1	SC	12	Hydrogen + Charging	23 (RT)	1.00	50	5A__	100
				23				50	5B__	
6 – Swage	Swaged	BS EN 1057	SC	12	Air	23 (RT)	1.00	10	6A_	60
					Hydrogen + Charging			10	6B_	
				23	Air			10	6C_	
					Hydrogen + Charging			10	6D_	
			None	CP 203	Air			10	6E_	
					Hydrogen + Charging			10	6F_	

4.4 Test Environments

The test environments were specified as follows:

1. **Air** - Samples tested in laboratory air, at room temperature (~23°C)
2. **Hydrogen** - Samples filled with gaseous hydrogen as detailed in Section 3.4. The regulator was set to 1 bar hydrogen and the internal pressure of the specimens is, as a result, assumed to be approximately 1 bar of gaseous hydrogen, however, it was not possible to verify this pressure or the hydrogen purity of the internal sample atmosphere.
3. **Charging** - Samples were immersion charged for 72 hours in a 20% ammonium thiocyanate solution as detailed in Section 3.3. It was not possible to experimentally quantify the levels of hydrogen absorbed during this process. Simplistic calculations and literature, as detailed in Annex A1, suggest the magnitude of absorbed hydrogen expected from this charging regime is to the order of 1-5 ppm.
4. **Hydrogen Charging** – Samples filled with gaseous hydrogen and immersion charged.
5. **Temperature** – Testing was conducted at room temperature as well as an elevated temperature of 50 °C. Testing at 50 °C was specified as the upper limit of the possible service temperature of jointed copper pipework. Testing at 'Temperature' is referring to testing at the elevated target temperature of 50 °C, this was achieved by setting the temperature controller on the environmental chamber shown in Figure 3.1 to 50 °C. The entry points into the chamber were packed with superwool for insulation. To first allow the chamber, accessories and grips to reach temperature, the environmental chamber was turned on one hour prior to testing, with a 50 °C target. Prior to each test, the sample was mounted into the grips and left to soak for ten minutes. The surface temperature of the sample for room temperature tests and tests at temperature (50 °C) was measured prior to test start using a type K thermocouple.

4.5 Data

4.5.1 Stress Calculations

The engineering stress has been calculated using the pipe cross sectional area. The pipe has a wall thickness of 0.70 mm as specified in BS EN 1057, with a wall thickness tolerance of ±10%, and an outside diameter of 15.00 mm, with a tolerance of ± 0.04 mm. In practice, where measured, the wall thickness tolerance was observed to be much smaller <5%. The error in the stress calculations incurred by making this assumption is reported in the processed data files. The force used for stress calculations is the force measured by the load cell output on the UTM.

4.5.2 Strain Calculations

The engineering strain has been calculated using the gauge length of each sample as measured by a set of vernier callipers to resolution of 0.1 mm. In this case, the gauge length has simply been measured as the length of the specimen between the two grips. The crosshead displacement was taken as the change in sample length. Strain throughout this report is referring to the engineering strain.

5 Results and Analysis

5.1 Data Analysis

Two characteristic points were identified for analysis, the UTS and 'failure'. Failure is defined here as the point at which a 10% drop from the UTS is realised, with their associated strains. These points have been labelled in Figure 5.1. The UTS was selected as this is the maximum load the specimen, and pertinently the joint, is able to withstand prior to failure. The selected 'failure' point is the point at which hydrogen leakage would occur. These two points have been extracted for each sample. These two points, specifically the UTS and failure strain have formed the basis of the analysis. This data, alongside other key sample data, have been collated into a spreadsheet; alongside the raw and processed data, which will be made available.

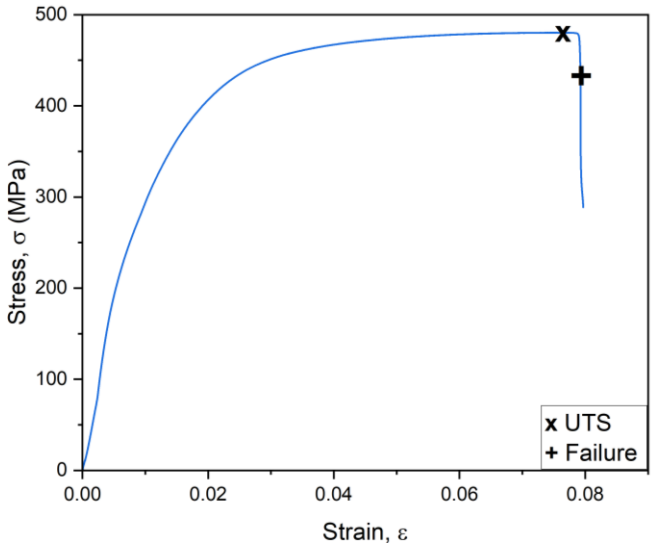

Figure 5.1 – Stress strain plot for sample 2D2, the key analysis points, the UTS and failure have been labelled.

5.2 Failure Modes

The jointed samples exhibit several different failure modes, as shown in Figure 5.2. This project (and hence the bulk of testing) has been focused on jointed samples. Coupler jointed samples contain three components, two sections of pipe and the coupler, with two interfaces making up the joint. For swaged samples there are two components, just the two sections of pipe, with one interface making up the joint. With the component nature of these samples, a mixed failure mode for jointed specimens was observed. The failure mode observed has been recorded for all samples and understanding the impact of the test environment on the frequency of the different failure modes is a key feature for analysis.

Failure at the joint was not observed for any of the brazed samples, attributed to the joint being stronger than the base copper pipe. The brazed joint is formed at much higher temperatures than the soldered joint and the brazing filler is predominantly copper based. As a result, the interface between the pipe and coupler is believed to be more coherent with the base material than the soldered joint. This more coherent interface facilitates load transfer through the sample, through the coupler, which can result in failure along the centre notch in the coupler. This coupler failure mode was not common for soldered samples, and was only observed in one soldered sample, 5B31, in the practitioner variability testing series. In this instance, excess solder had been applied connecting the two interfaces with a continuous span of solder, facilitating load transfer through the coupler, and resulting in coupler failure.

For swaged joints, in addition to the basic pipe and joint failure modes, near joint failure has also been designated, as observed in Figure 5.2 D(ii). This is pipe-based failure that occurs circumferentially along the swage line, the point at which the pipe has been deformed to create the fitting. Swaged joints were made by hammering a socket forming tool into the pipe which deforms the pipe, this process will result in work hardening of the copper, introducing defects which may act as a source of failure. Five of the 60 swaged samples failed in this manner. Rotary swaging devices are available which would likely reduce work hardening and in turn, reduce the likelihood of this failure mode.

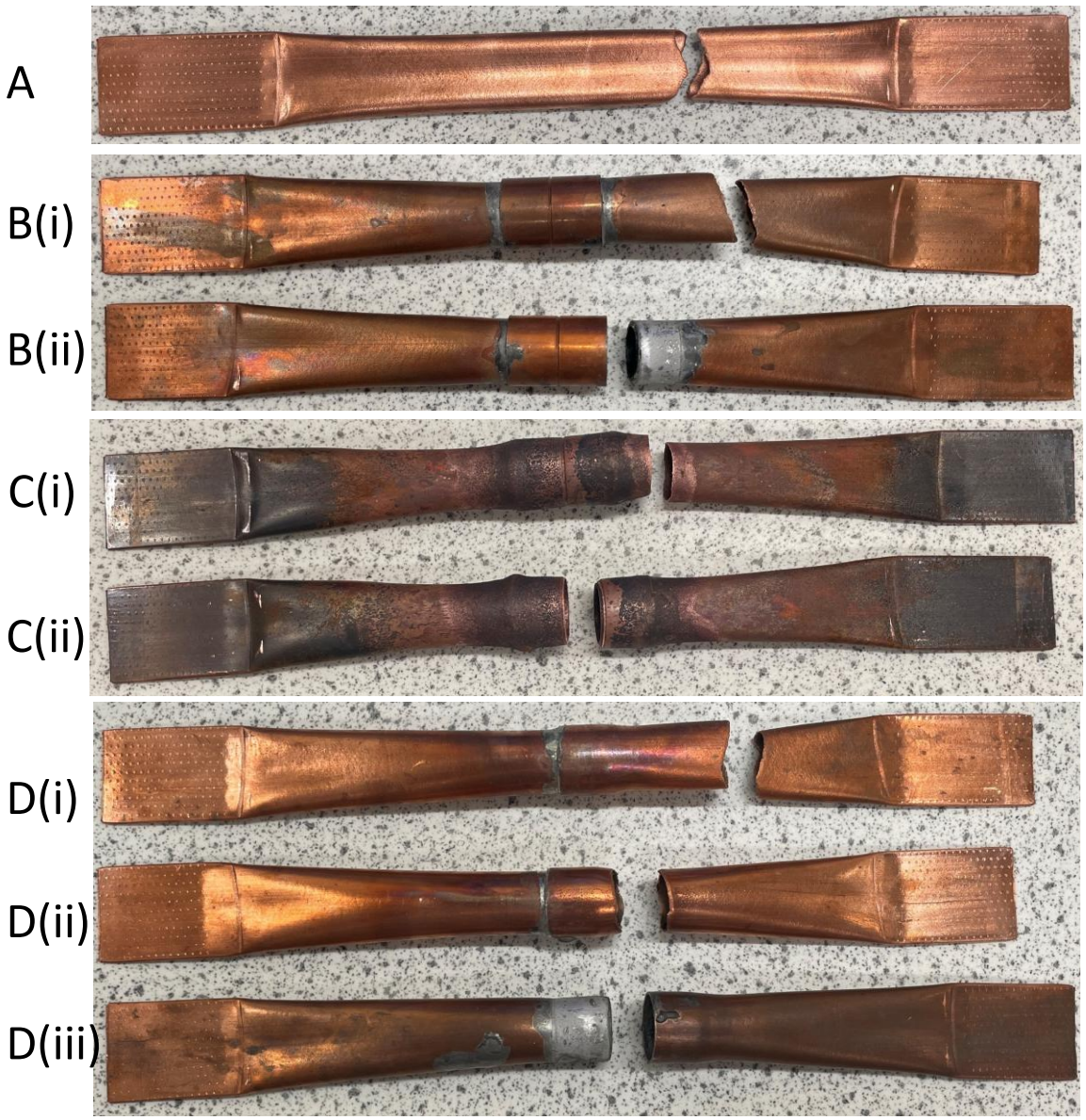

Figure 5.2 – Failure modes for specimens for: A, pipe failure; B, soldered coupler joints for (i) pipe failure and (ii) joint failure; C, brazed coupler joints exhibiting (i) pipe failure and (ii) coupler failure; and D, swaged joints with (i) pipe failure, (ii) pipe – near joint failure, and (iii) joint failure.

5.3 Gauge Length

As the samples were crimped and gripped manually, there was significant variation observed in the gauge length, ranging from 93.2 mm to 147.1 mm. The variation of UTS with gauge length can be seen in Figure 5.3 A, and the variation of strain at failure with gauge length in Figure 5.2 B. Both UTS and strain at failure appear to be insensitive to gauge length with neither variable exhibiting any significant correlation.

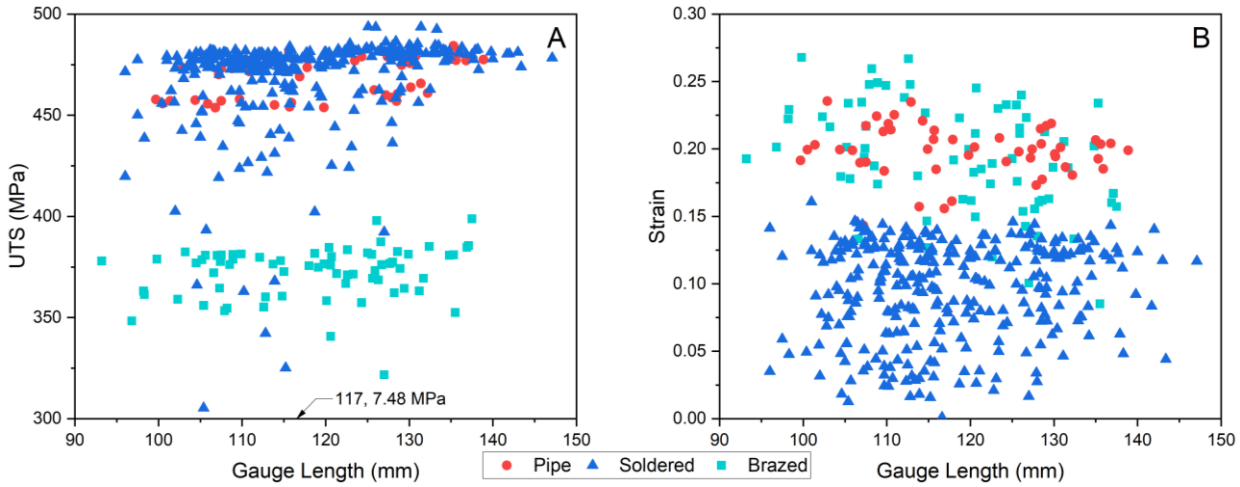

Figure 5.3 – Variation with specimen gauge length for: A, UTS stress, and, B, strain at failure. Data has been segregated into pipe, soldered, and brazed samples.

5.4 Temperature

Testing was conducted at two different temperatures: room temperature (at which the majority of samples were tested) and a target temperature of 50 °C (achieved using an environmental chamber). The sample temperature was measured with a thermocouple prior to testing, and samples temperatures were recorded as 21.6 to 25.9 °C when testing at room temperature, and 46.0 °C to 54.0 °C when testing at elevated temperature. The variation of UTS with temperature can be seen in Figure 5.4 A, and the variation of strain at failure with temperature in Figure 5.4 B. There is a clear reduction in both UTS and strain at failure for soldered samples as temperature increases.

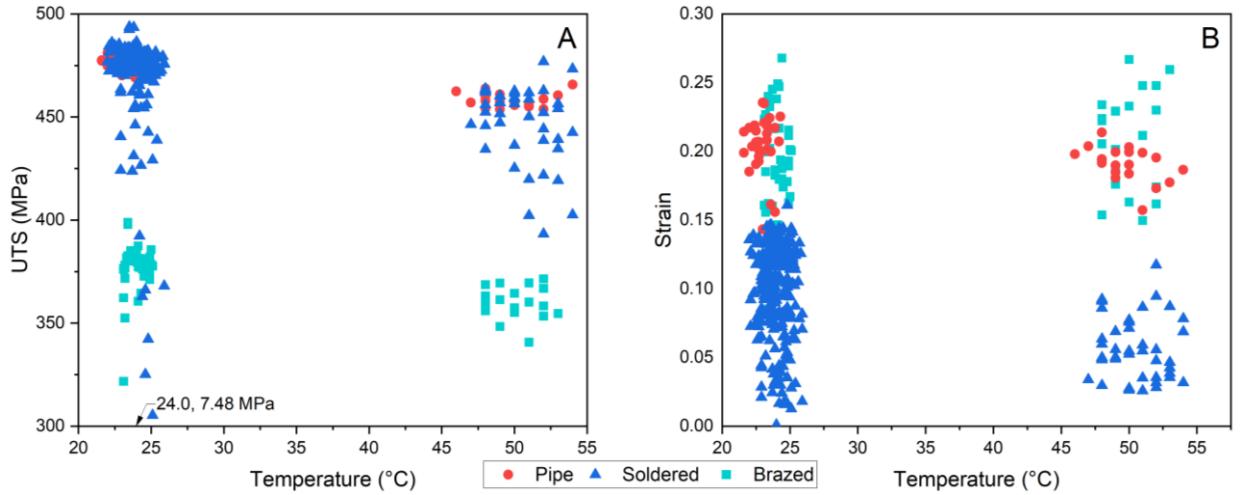

Figure 5.4 - Variation of data with sample temperature with: A, UTS stress, and, B, strain at failure. Data has been split up into pipe, soldered, and brazed samples.

5.5 Data Presentation

Box and whisker plots have been used to present the data series for samples tested at an extension rate of 1.00 mm/min, facilitated by the 10 samples within each series with unique test condition and specimen type. Standard box and whisker plots have been used. The box extending from the lower to upper quartile; the whisker range defined as 1.5 the interquartile range; the median, mean, and outliers are labelled. The formatting and symbols of the box and whisker plots, and corresponding legend are shown in Figure 5.5; this legend is applicable to box plots used throughout this report. No results have been excluded from the box and whisker plots and associated median, mean, and range calculations. The UTS and strain at failure data extracted from the force displacement data has been collated for all series and this data forms the basis for the box and whisker plots.

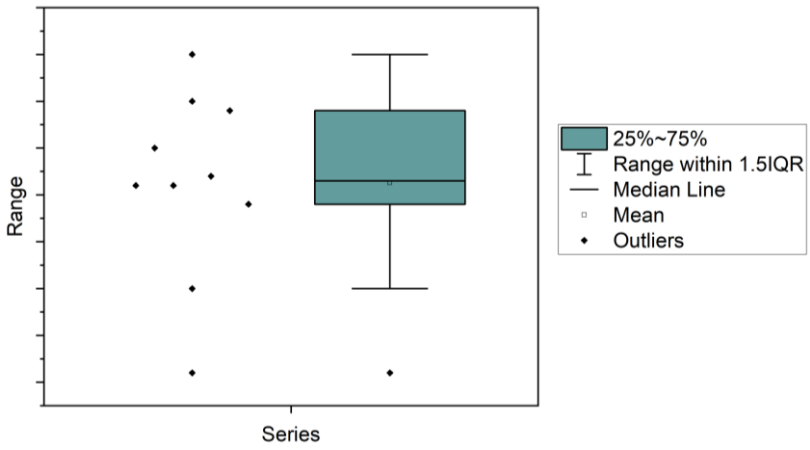

Figure 5.5 – Example box and whisker plot, the individual data points are plotted to the left of the box and whisker.

5.6 Pipe-only Samples

Whilst the focus of this project is on the soldered and brazed joints in copper pipework, 50 pipe-only specimens have been tested to understand the properties of the base 15 mm copper pipework and the impact hydrogen can have. As observed in Figure 5.6 A, hydrogen charging results in a small decrease in the UTS measured over the series, where baseline tests in air are series 1A (room temperature) and series 1B (at elevated temperature). Testing at elevated temperature results in a decrease in UTS for both testing in air and hydrogen. Testing in hydrogen had no significant impact on strain at failure (Figure 5.6 B), although the spread in the data for series 2B for hydrogen charging is greater than the baseline series 1A. However, this increase in variation is not observed at elevated temperature for series 3A relative to 1B.

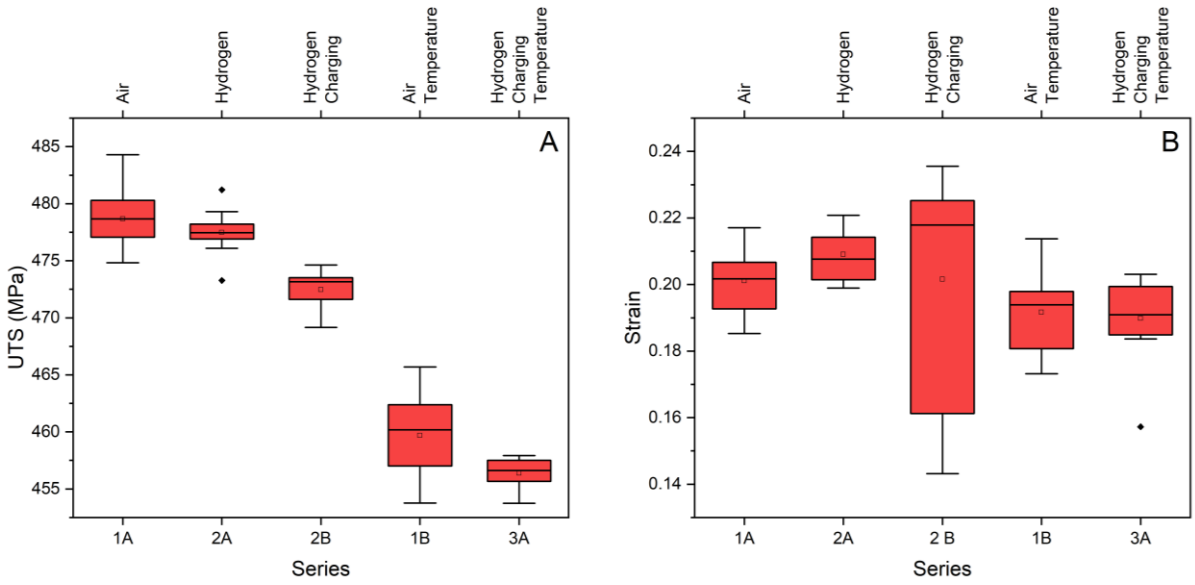

Figure 5.6 – Box and whisker plots comparing the extracted pipe series data over different test environments. A, UTS and B, strain at failure.

5.7 Soldered Samples

5.7.1 Alloy 12

The UTS and strain at failure series data for soldered coupler joints made with alloy 12 and self-cleaning flux is captured in Figure 5.7. As observed in Figure 5.7 A, the UTS for samples at room temperature (series 1C, 2C, and 2D) is similar to the equivalent pipe only samples in Figure 5.6 A, suggesting that the UTS and loading is dominated by the base 15 mm copper pipe and not the soldered joint. There is a slight reduction in UTS for the hydrogen charging series 2D relative to its baseline series 1C, consistent with the pipe samples. For the series tested at room temperature, a mixed mode failure was observed, whereas while testing at elevated temperature, the specimens failed at the joint.

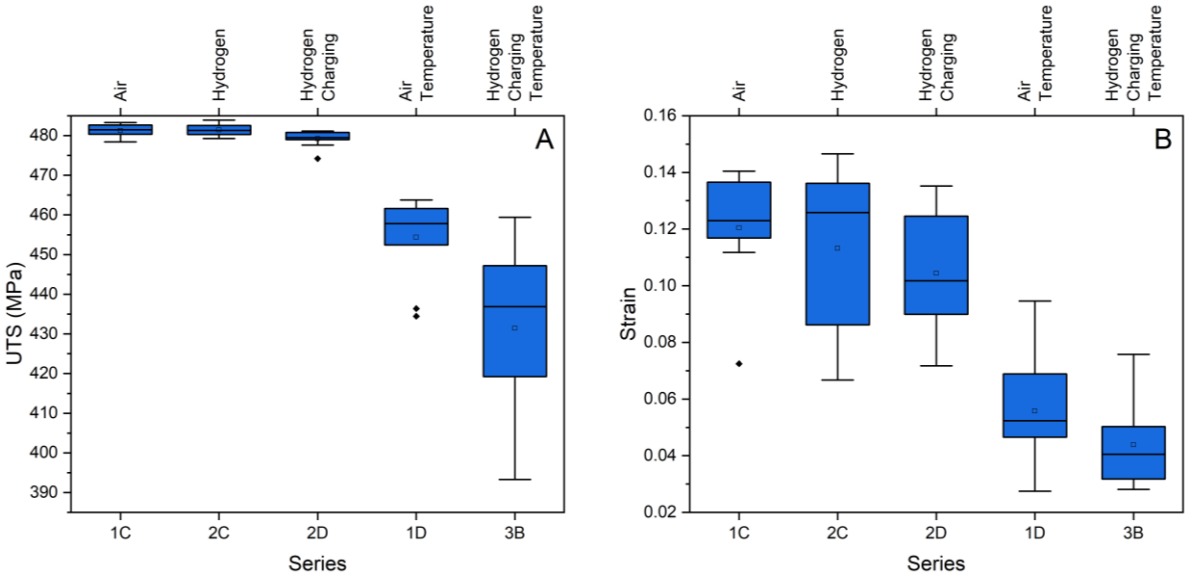

Figure 5.7 – Box and whisker plots comparing the extracted series data for soldered coupler specimens made using alloy 12 and self-cleaning flux over different test environments. A, UTS and B, strain at failure.

5.7.2 Alloy 23

The UTS and strain at failure data for soldered coupler joints made using solder 23 and self-cleaning flux, shown in Figure 5.8, exhibit comparable properties to soldered joints made with solder 12, as previously discussed. Again, testing at elevated temperature resulted in a transition from a mixed failure mode between the pipe and joint to jointed only failure.

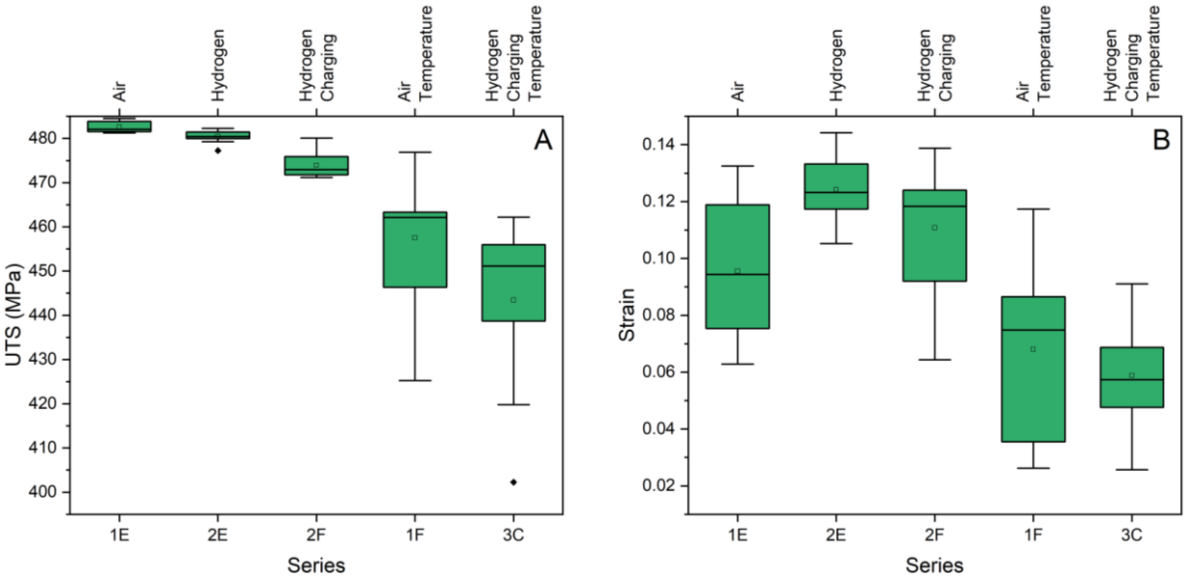

Figure 5.8 – Box and whisker plots comparing the extracted series data for soldered coupler specimens made using alloy 23 and self-cleaning flux over different test environments. A, UTS and B, strain at failure.

5.7.3 Flux Comparison

Self-cleaning flux was used for the majority of the soldered joints in this project and is the standard choice in the UK. Soldered joints made using tinned flux were also tested; tinned flux contains small solder particles. No tinned flux to the required ASTM B813 standard could be located in the UK and the tinned flux used was imported from the US. The tinning flux procured contains a leaded solder. Tinned flux does not appear to be used in the UK and no evidence of its historic use could be found, however, it is widely used in the US. The results of the tinned flux series are plotted alongside comparable self-cleaning flux series for UTS in Figure 5.9 and strain at failure in Figure 5.10.

As observed in Figure 5.9, the UTS for all four solder and flux combinations is similar. The gaseous hydrogen test environment made no significant difference relative to the baseline testing in air. A slight decrease in the UTS for the hydrogen charging test environment is observed for all four solder flux combinations. For all four solder combinations the UTS and loading behaviour up to the UTS is very similar, this is believed to support the prior observation that the UTS and loading appears to be dominated by the base 15 mm copper pipe and not the soldered joint. The combination of materials used to make the soldered joint has not been measured to have any significant impact on the tensile properties of the specimens as tested. All series exhibited mixed mode failure with no consistent correlation for hydrogen or hydrogen and charging to increase the propensity of specimens to fail at the pipe or joint. Observing Figure 5.10, the strain at failure is similarly comparable for all four solder flux combinations in each series, within each test environment; hydrogen or hydrogen and charging have no significant impact on strain at failure. Series 1H, 2G, and 2J each contain a data point with abnormally low UTS and strain at failure, all these specimens were a jointed failure. These results have not been excluded from the box and whisker range, mean, and median calculations. These three abnormal results come from joints made using a tinned flux. Following inspection, it is believed to be as a result of joint quality and failure for solder to fully infiltrate the joint interface, rather than due to the flux choice.

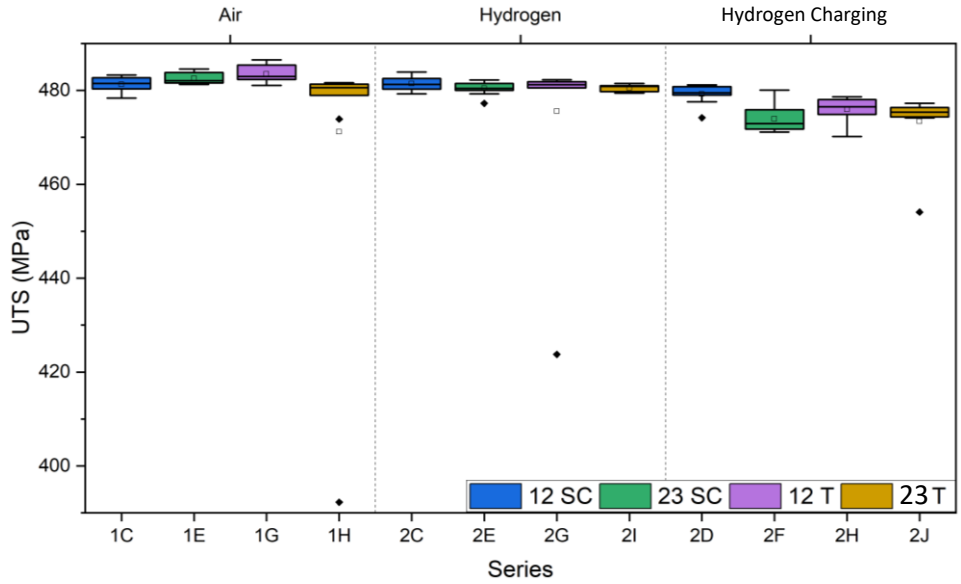

Figure 5.9 – Box and whisker plot comparing the extracted UTS data for all room temperature series of soldered coupler specimens. Specimens made using four different solder and flux combinations as per figure legend, with SC referring to self-cleaning flux and T referring to tinned flux, 12 and 23 referring to alloys 12 and 23, respectively. Series have been grouped by test environment.

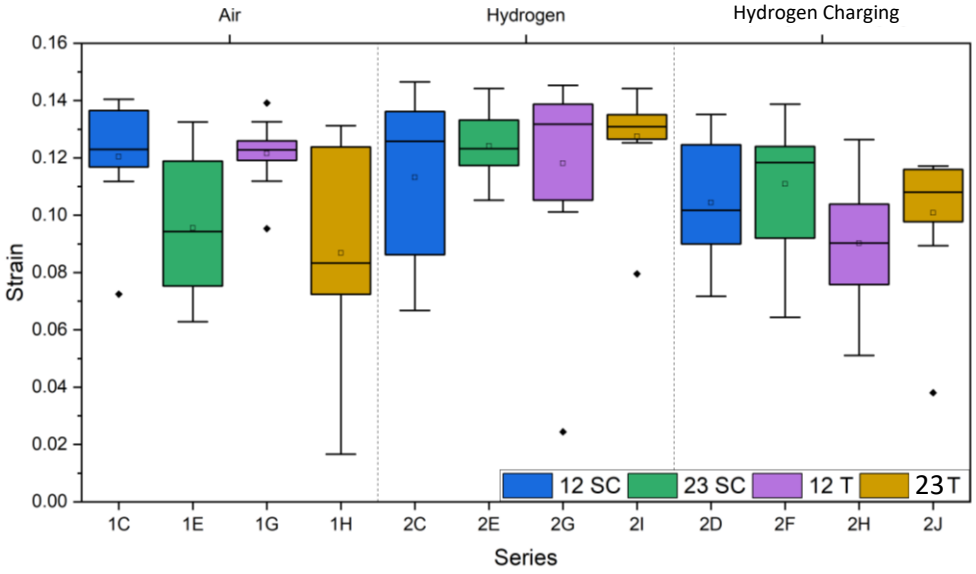

Figure 5.10 – Box and whisker plot comparing the strain at failure data for all room temperature series of soldered coupler specimens. Specimens made using four different solder and flux combinations as per the figure legend, with SC referring to self-cleaning flux and T referring to tinned flux, 12 and 23 referring to alloys 12 and 23, respectively. Series have been grouped by test environment.

5.8 Brazed Samples

The tensile response of brazed samples differed from the soldered specimens, reaching an approximately 20% lower UTS value and failing at approximately double the strain. Brazed specimen failure modes are captured in Figure 5.2 and Section 5.3. The brazed specimens exhibited mixed mode failure in all test conditions, split between pipe and coupler-based failure, with no consistent correlation to test environment on failure mode. Figure 5.11 A shows the UTS of the brazed specimens decreases relative to its respective air baseline series for hydrogen charging at room and elevated temperature. There is no clear impact of test environment on strain at failure (Figure 5.11 B).

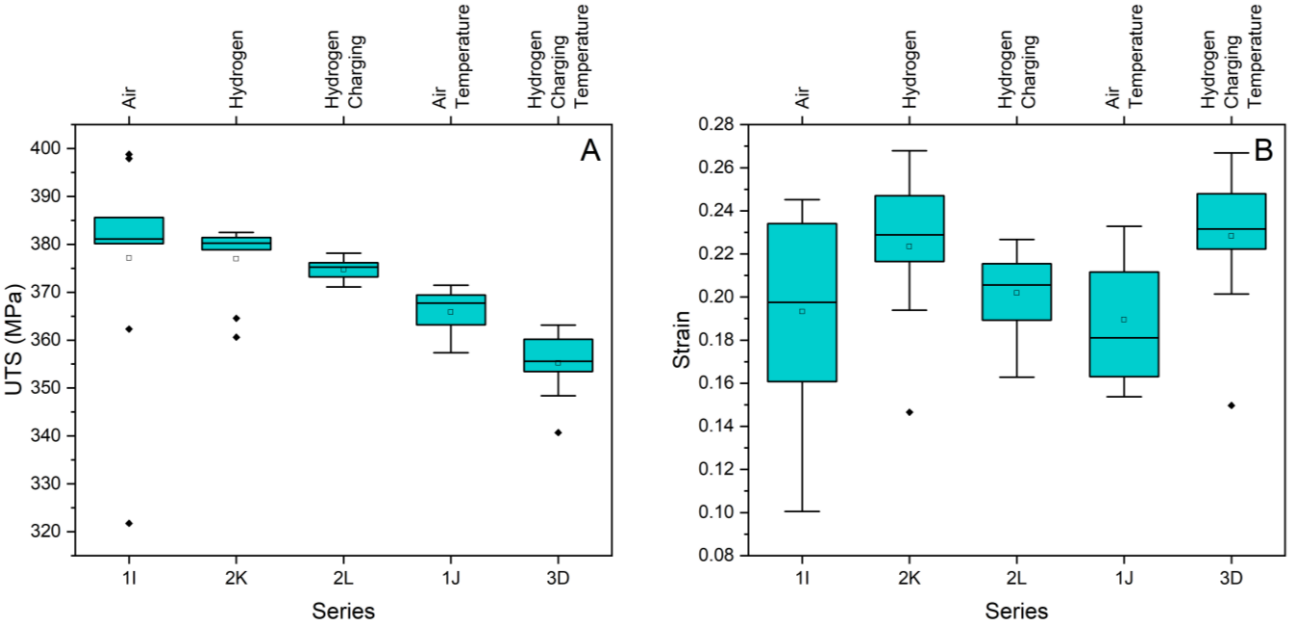

Figure 5.11 – Box and whisker plots for the extracted data for all brazed coupler specimen series. Specimens made using the CP 203 braze filler. A, UTS and B, strain at failure.

5.9 Swaged Samples

The UTS and strain to failure of the swaged samples, as plotted in Figure 5.12 A and 5.12 B respectively, behave similarly to the equivalent coupler jointed series. Hydrogen charging resulted in a slight reduction in UTS, and no clear trend in strain to failure. The swaged brazed samples (CP 203), were consistent with the brazed coupler series, no jointed failure was observed, with failure occurring at the pipe, or at the pipe – near joint. Hydrogen and hydrogen charging had no clear impact on failure mode for either the soldered or brazed swaged specimens. The soldered swaged series (solder 12 and 23) exhibited mixed mode failure in both test conditions, with failure occurring in the pipe, pipe – near joint, and at the joint.

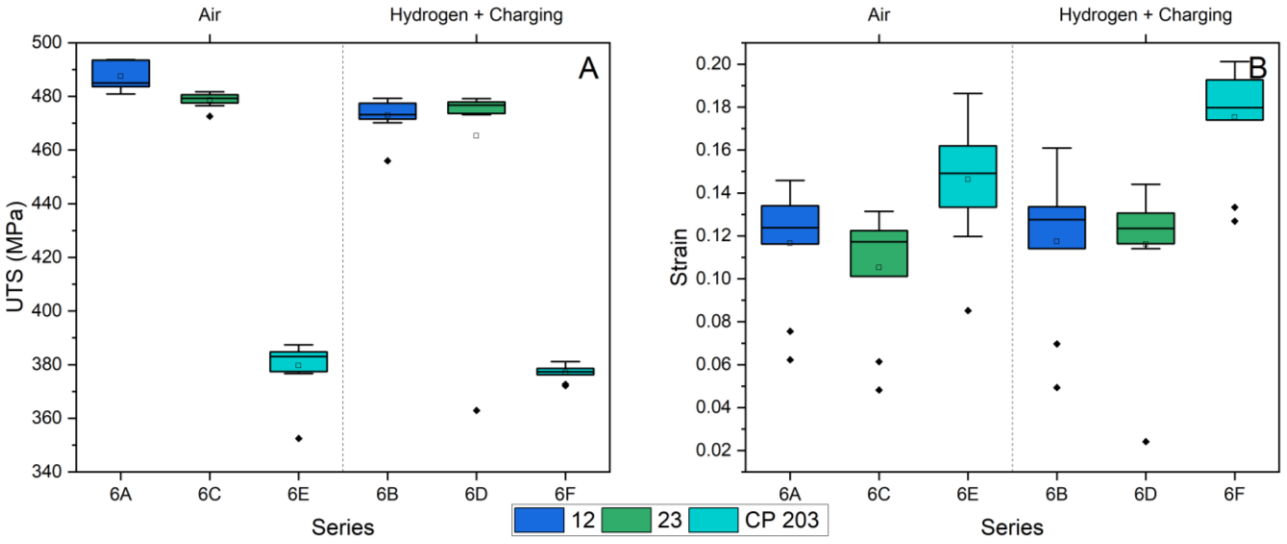

Figure 5.12 – Box and whisker plots comparing the extracted data for all swaged specimen series. Specimens made using three different materials as per the figure legend, with 12 and 23 referring to alloys 12 and 23 respectively, and CP 203 for brazed samples. Series have been grouped by test environment. A, UTS and B, strain at failure.

5.10 Practitioner Variability

To assess the variability of soldered joints in a hydrogen and hydrogen charged test environment, five different trained at plumbers at Fareham Plumbing and Heating Ltd prepared two series each of coupler soldered samples. One using alloy 12 and the other using alloy 23, both using the self-cleaning flux. With the exception of the practitioner variability series, for consistency, all soldered specimens were made by one plumber. The UTS data from the series is plotted in Figure 5.13 and the strain at failure data in Figure 5.14. The series labels are structured such that series 5A1 and 5B1 are made by the one practitioner, series 5A2 and 5B2 are made by another practitioner, and so on.

With the exception of series 5B1, the practitioner variability series exhibit similar behaviour to the relative core testing series. Both UTS and strain at failure for both solder 12 and solder 23 exhibit similar values and distributions.

In series 5B1, 90% of the specimens failed at the joint, which is higher than any other series tested. Typically, the frequency of soldered joints failure at the joint at room temperature was between 20 and 60%; the failure mode split for all other practitioner variability series is in line with the other core testing series at room temperature. Inspection of the 5B1 series joints, clearly showed that the solder has not fully infiltrated the joint, thus reducing the area of the interface and as a result, reducing joint strength. This phenomenon explains all results throughout all testing where an unexpectedly low UTS or strain was observed. Whilst the UTS and strain was reduced relative to the other practitioner variability series, the mean UTS is still fairly high with a value of 410 MPa.

In series 5A4 there was one specimen with an exceptionally low UTS of 7.48 MPa; in this extreme example little to no solder infiltrated the interface between the pipe and the coupler, resulting in a weak joint. This sample was filled with hydrogen to 1 bar through the process detailed in Section 3.4, and no leak was detected from the joint prior to testing.

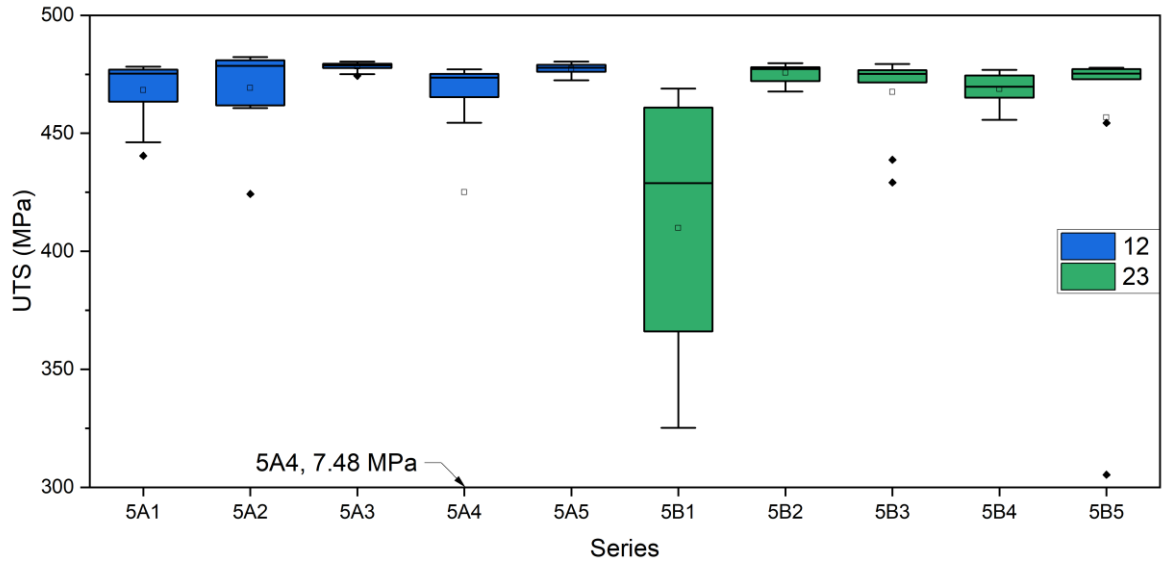

Figure 5.13 – Box and whisker plot comparing the extracted UTS data for the practitioner variability series testing. Specimens have been grouped by the solder used with specimens made using two different solders as per the figure legend, with 12 and 23 referring to alloys 12 and 23, respectively. All samples in the practitioner variability series of testing were tested in gaseous hydrogen and underwent hydrogen charging.

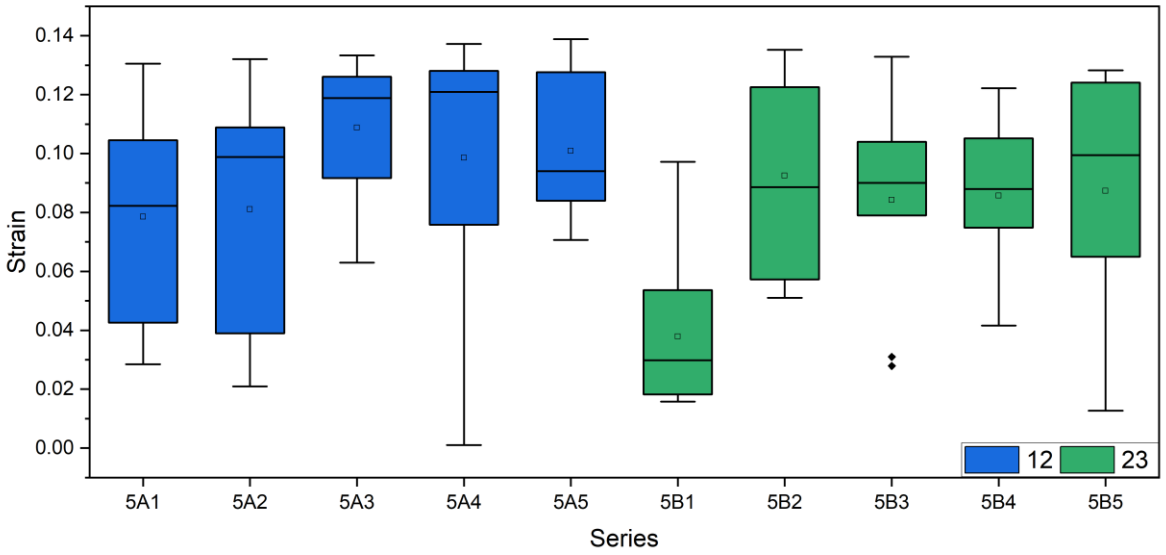

Figure 5.14 – Box and whisker plot comparing the extracted strain at failure data for the practitioner variability series testing. Specimens have been grouped by the solder used with specimens made using two different solders as per the figure legend, with 12 and 23 referring to alloys 12 and 23, respectively. All samples in the practitioner variability series of testing were tested in gaseous hydrogen and underwent hydrogen charging.

5.11 Slow Strain Rate Testing

For the slow strain rate testing, all soldered specimen tests failed at the joint, and all brazed specimens failed in the pipe. This is contrast to the faster strain rates testing results, where both soldered and brazed samples exhibited mixed mode failure, soldered samples failed at the pipe and joint, and brazed samples failed at the pipe and coupler.

5.11.1 Test Duration

The strain behaviour of slow strain rate tests of brazed samples at extension rates of 0.10 mm/min and 0.01 mm/min is similar to the brazed sample strain at 1.00 mm/min. This can be observed in Figure 5.15 B for both air and hydrogen, with all three stress strain curves loading up to and eventually failing at similar points. The soldered samples did not behave in this manner, with the specimens tested at slower extension rates failing at a significantly lower UTS and strain in both air and hydrogen, as can be seen in Figure 5.15 A.

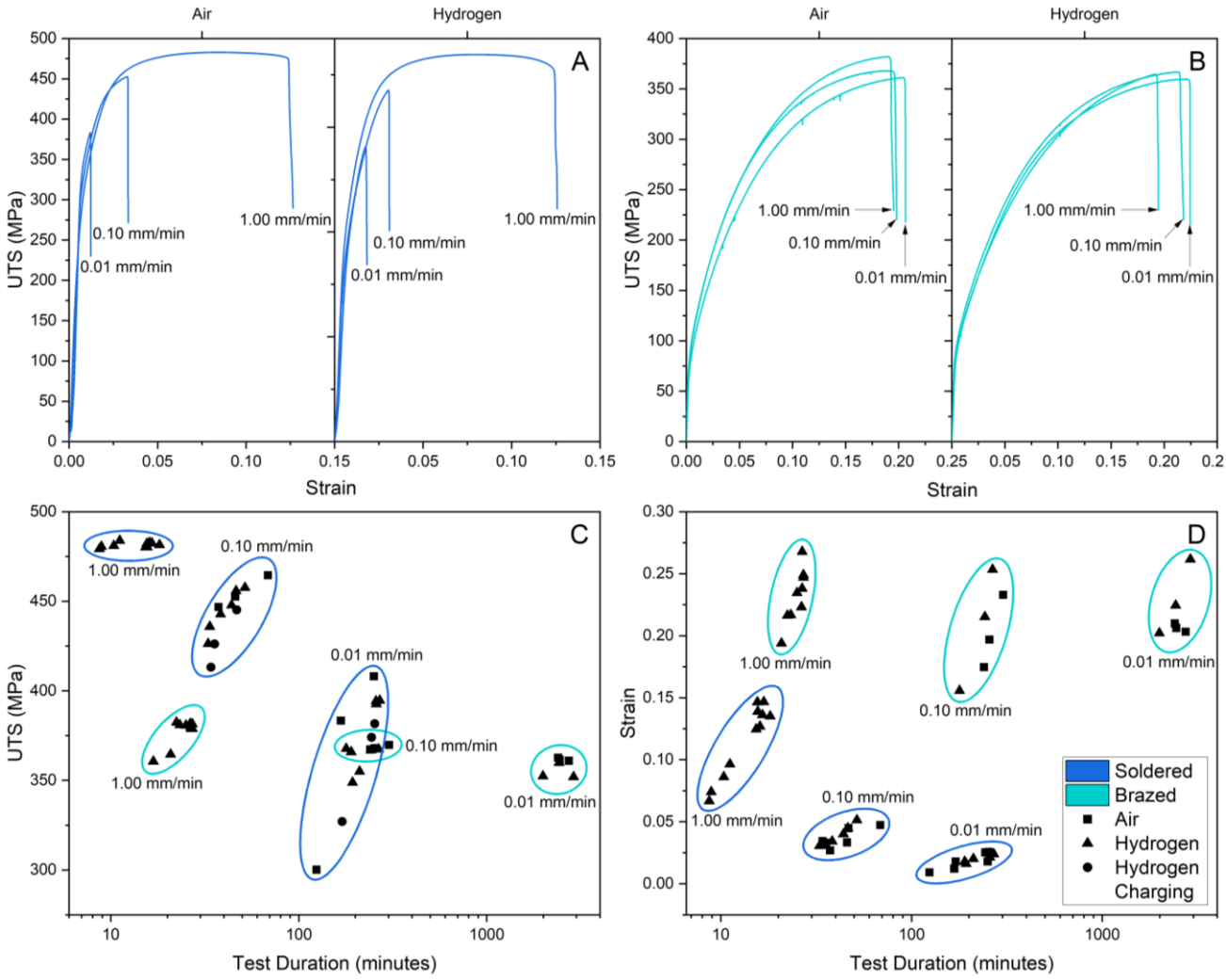

Figure 5.15 A & B – Stress-strain curves for the tests at different strain rates for median strain at a failure samples. A, soldered samples, made using alloy 12 solder and self-cleaning flux. B, brazed samples, grouped into air and hydrogen. The specimen within each respective series with the median strain at failure value is plotted. C & D – Extracted data for all slow strain rate test series and a relevant series at highest strain rate tests, plotted against test duration. C, UTS data; D, strain at failure data.

The test duration scaled linearly, as expected for the brazed samples, with tests at extension rates of 0.10 and 0.01 mm/min taking approximately ten and 100 times longer than the 1.00 mm/min extension rate tests respectively. The stress strain curves are similar and as a result, and as depicted in Figure 5.15 A-D, the UTS and strain at failure for the brazed samples is relatively insensitive to extension rate for the three different extension rates tested in both air and hydrogen test environments. The soldered samples, however, at lower extension rates failed at lower strains and

lower stresses in both air and hydrogen test environments. This results in a reduced test duration relative to the extension rate, relative to the expected increase. As shown in Figure 5.15 A-D the UTS and strain at failure decreases as test duration increases and extension rate decreases for soldered samples but not for brazed samples.

Slow strain rate hydrogen testing aims to increase the time under tension, facilitating hydrogen absorption to give a measure of resulting embrittlement. As the soldered joints demonstrated accelerated failure at slower strain rates, in both air and hydrogen, the time under tension may not have been sufficient to give an indication of the resulting embrittlement. Tests at an extension rate of 0.01 mm/min lasted an average of 216 minutes for soldered samples but an average of 2480 minutes for the brazed samples.

5.11.2 Soldered Samples

The slow strain rate testing of the soldered samples (alloy 12 and alloy 23) are shown in Figure 5.16. Based on the similar performance of these two solders at the faster extension rate of 1.00 mm/min (shown in Figure 5.14), it has been assumed that, for the purposes of this test work, the baseline testing of alloy 12 at slower strain rates (series 4A and 4B) is a suitable baseline for alloy 23 slow strain rate testing (Series 4E-4H). Baseline testing in air was therefore only conducted for alloy 12 soldered samples and not for alloy 23.

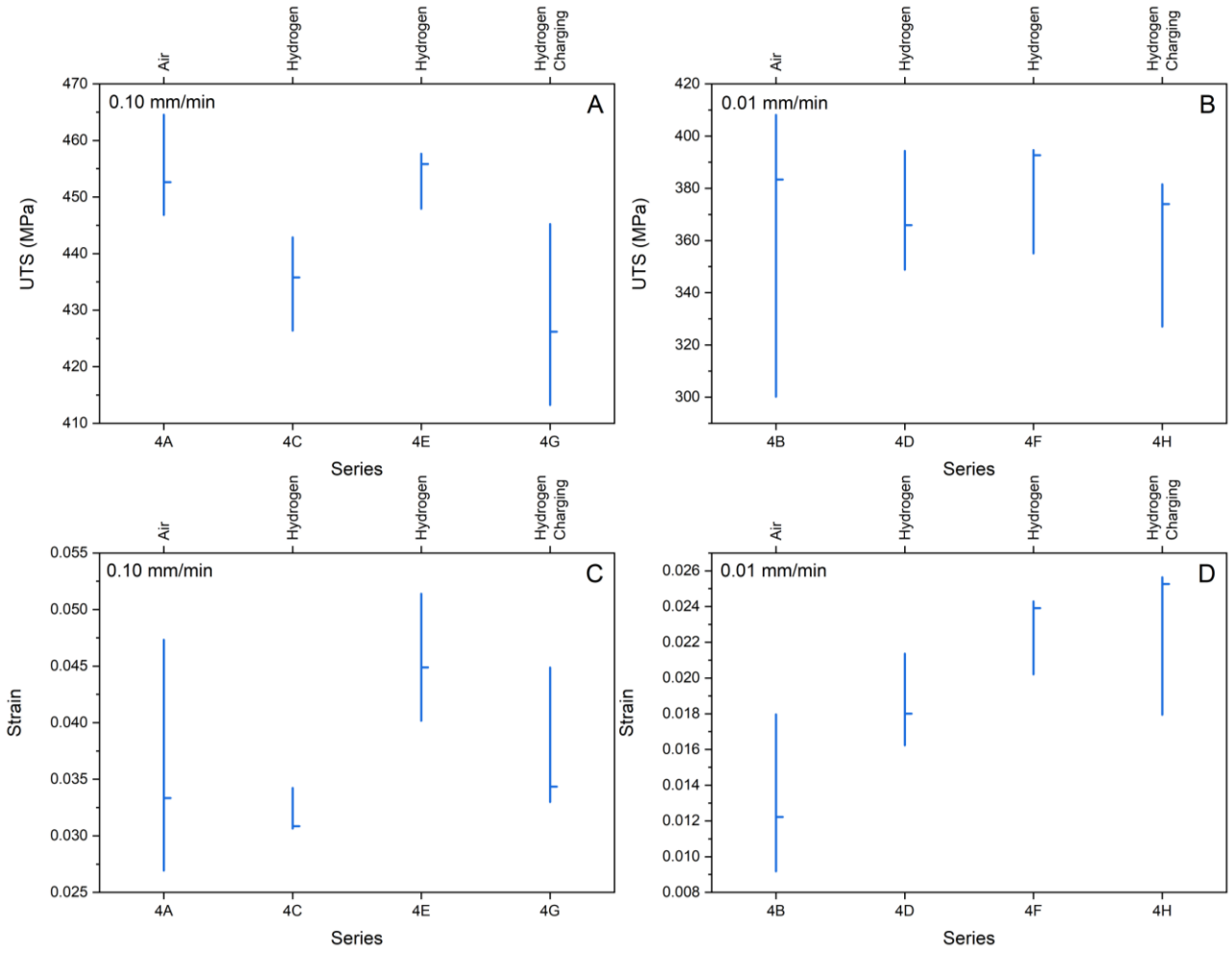

Figure 5.16 – Extracted UTS and strain at failure data for each series of soldered specimen slow strain rate testing. Each series of three data points plotted, with the top of the line one data point, the bottom another, and the horizonal protruding line the final data point. Series 4A-4D are made with alloy 12 and series 4E-4H are made with alloy 23. A, 0.10 mm/min UTS. B, 0.01 mm/min UTS. C, 0.10 mm/min strain at failure. D, 0.01 mm/min strain at failure.

The UTS of soldered samples at an extension rate of 0.10 mm/min is plotted in Figure 5.16 A. The tests conducted in gaseous hydrogen have a lower mean UTS than the baseline series 4A, this decrease is larger for alloy 12 (series 4C) than alloy 23 (series 4E). Alloy 23, when hydrogen charged and filled with gaseous hydrogen (series 4G), gives a larger reduction in UTS relative to the equivalent baseline. A reduction in UTS, relative to the baseline series 4B, at an extension rate of 0.01 mm/min is not seen for specimens tested in hydrogen environments (Figure 5.16 B). There is no clear correlation in strain to failure under the different test environments at either the extension rates of 0.10 or 0.01 mm/min (Figure 5.16 C&D).

5.11.3 Brazed Samples

The UTS and strain to failure data for brazed coupler joints for slow strain rate testing are plotted in Figure 5.17. There is a small, measured decrease in UTS for tests at extension rates of both 0.10 and 0.01 mm/min in hydrogen, relative to the baseline in air. The decrease is small and an overlap in the series UTS data makes it is difficult to suggest, considering this small dataset, whether this decrease is caused by the hydrogen test environment. There is no clear impact of hydrogen on the strain at failure.

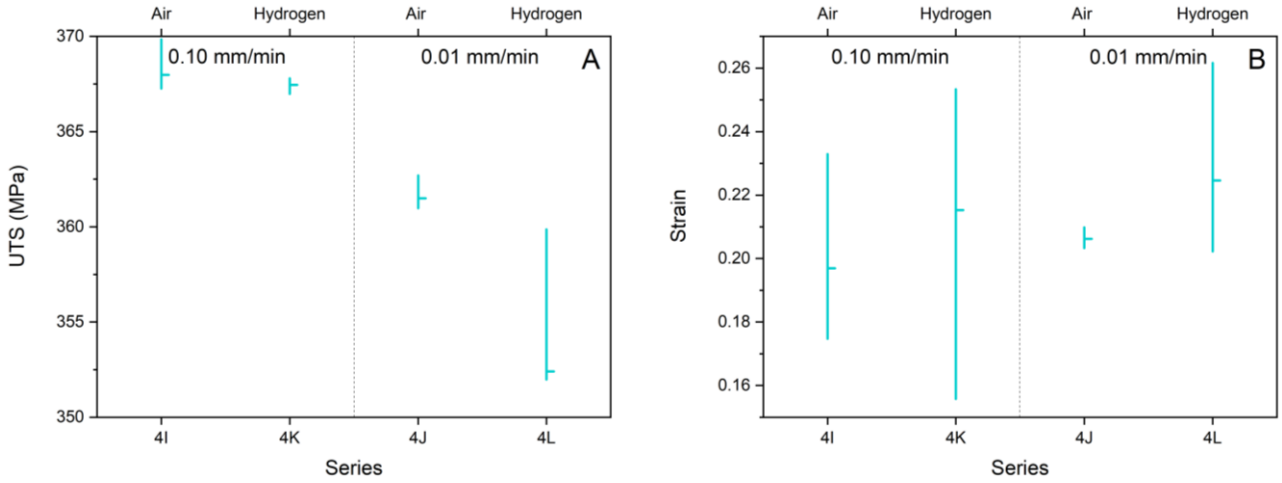

Figure 5.17 – Extracted data for each series of brazed specimen slow strain rate testing. A, UTS and B, strain at failure. Each series of three plotted, with the top of the line one data point, the bottom another, and the horizonal protruding line the final data point. Series grouped by extension rate as labelled.

5.12 Weibull Analysis

5.12.1 Process

Weibull statistics is an approach that has application wherever there is a population of samples needing to be compared. In the context of Materials Science and Engineering, it is used whenever there is a need to consider a population which is known to contain defects that will impact on performance, or where such defects are suspected.

The first step to interrogate a data set is to determine a probability of occurrence. There are several routes to calculating this probability, with the consistent feature being that the samples are ranked in order of magnitude from smallest to largest. The position order and the total number of specimens in the set then form the basis of the Equation 5.1:

$$P_s = \frac{j-\frac{3}{8}}{N+\frac{1}{4}} \qquad 5.1$$

Where P_s is the probability of survival, j is the rank within the set, and N is the number of samples in the set. Hence, for the third ranked sample in a set of ten, the probability of survival would be:

$$P_S = \frac{3-\frac{3}{8}}{10+\frac{1}{4}} = \frac{2.625}{10.25} = 0.256 \quad 5.2$$

A Weibull plot is then produced by comparing $\ln \ln \left(\frac{1}{1-P_S}\right)$ with ln (W), where W is the property of interest. By fitting a straight line through the data, two properties can be determined: W_0 is the characteristic value of the property W, and m is the Weibull modulus. The characteristic value has no special significance with respect to any mechanism of failure, or any physical characteristic. Rather, the characteristic value represents the point at which $\ln \ln \left(\frac{1}{1-P_S}\right)$ is 0, or to put it another way, Ps = e, and 37% of samples will be greater than the characteristic value, and 63 % smaller.

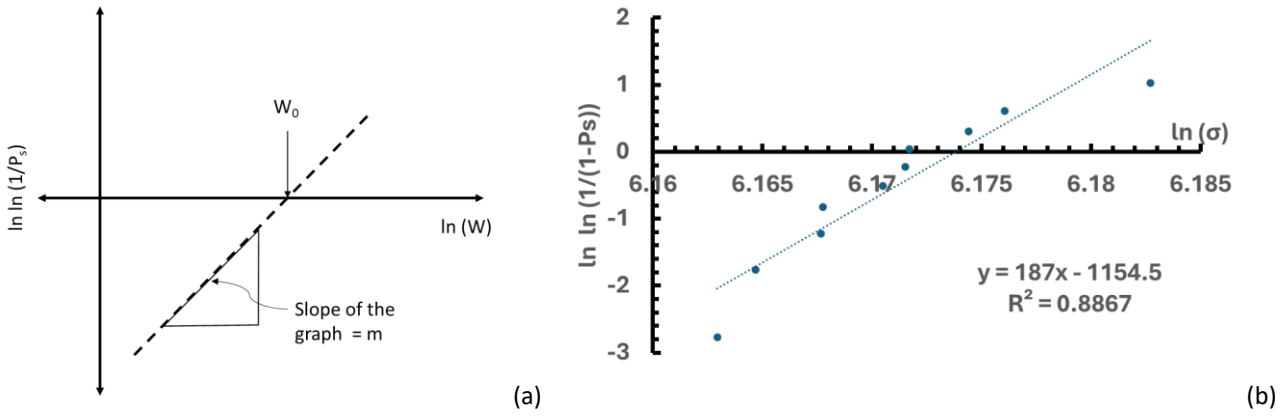

Figure 5.18 – Examples of a Weibull plot (a) labelled example demonstrating the method and (b) example Weibull plot for series 1A.

In the context of this study, it is the UTS which is of interest, and hence σ_0 will be determined using the measured UTS. The significance of the two properties, the Weibull modulus (m) and the characteristic strength (σ_0), are that for a single set of specimens, a behaviour for a joint in a pipe can be defined. Where m ≥ 100, the distribution of failure stresses is so narrow, it can be taken to be unique. The smaller m is, the broader the spread of values. Hence, it might be expected that a large value of m for the as-received joints is seen (assuming they are made consistently), and that there are no other factors to be considered. In comparison, the samples that have been pre-charged with hydrogen might either demonstrate a broader spread of values, with a small(er) m, representing a range of induced defects, or they might in fact lead to a narrower distribution than the reference set, if the impact of the pre-charging is to cause uniform damage, superseding any existing defect population. However, the σ_0 would be expected to fall, if either the pre-charging or hydrogen atmosphere is impacting on the performance of the pipe.

5.12.2 Analysis of Results

A Weibull analysis has been conducted for all test series with an extension rate of 1.00 mm/min. The ten data points for each unique test condition and specimen combination facilitates this analysis. The slow strain rate testing consists of three samples for each series, which is insufficient to conduct a Weibull analysis.

Using the extracted UTS data of each sample, a Weibull analysis for each series has been conducted. The UTS has been selected as the variable to be analysed as hydrogen appears to have a more consistent impact on the UTS than the strain or stress at failure. The full set of Weibull analysis for all series will be made available. Annex A2 contains for each series, the Weibull modulus (m), characteristic strength (σ_0), and the R squared measure for the linear equation fit to the dataset from which these properties are derived.

The Weibull series for all test series tested at room temperature at an extension rate of 1.00 mm/min is plotted in Figure 5.19. The tensile behaviour of soldered and brazed samples, as previously discussed, were found to differ, with

the Weibull series for brazed samples and the Weibull series for soldered samples clustering together. For the pipe and soldered specimens on the right-hand side of the figure, a negligible effect of hydrogen is observed within all series, regardless of their test environment, and appear relatively uniform in terms of behaviour. Similarly, for the CP 203 brazed series, there is no consistent impact of hydrogen.

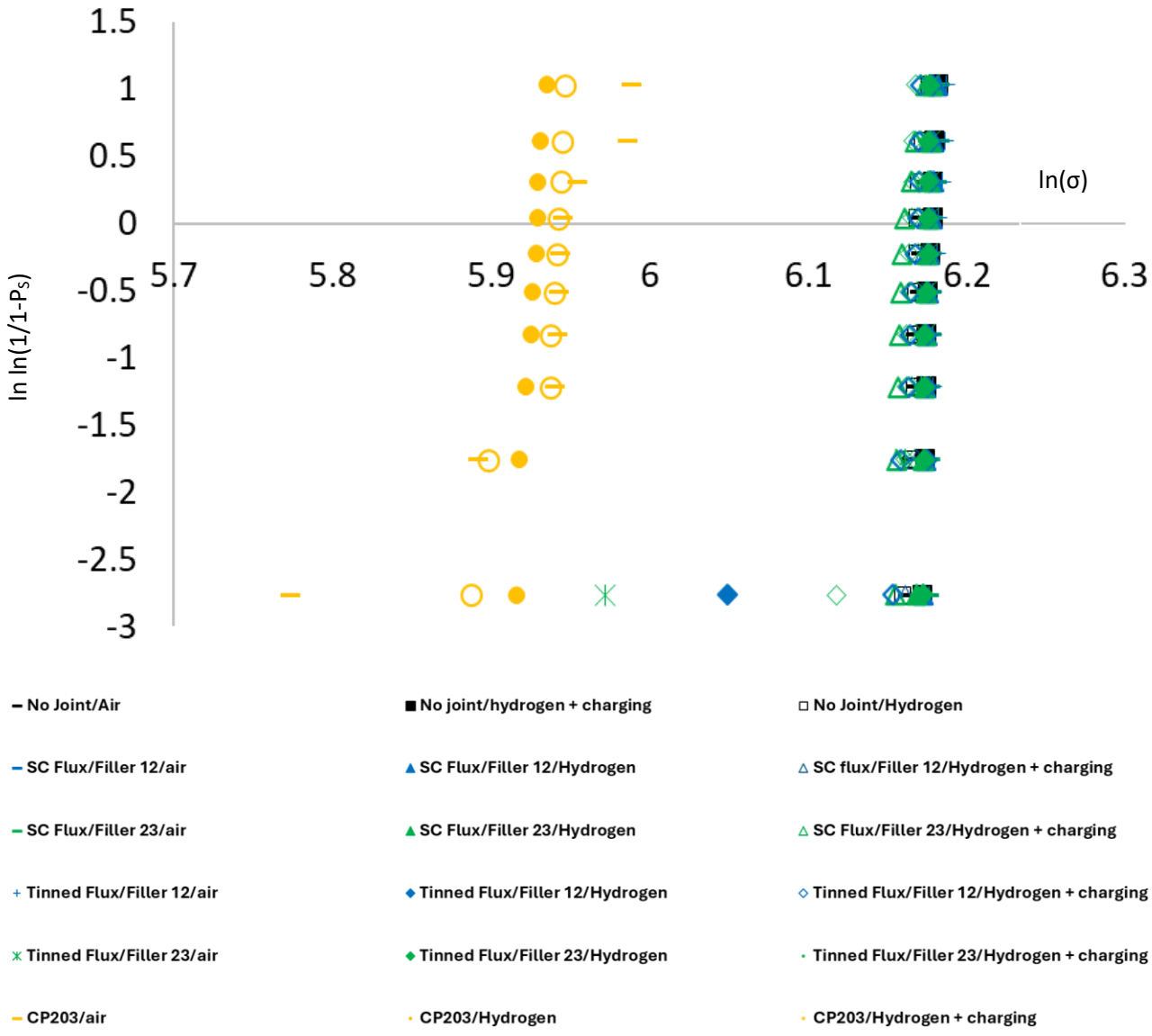

Figure 5.19 – Summary of all Weibull plots for series tested at room temperature at an extension of 1.00 mm/min. (For individual comparison, each series is presented as individual plots in Figure A.2 in Appendix 2).

In Figure 5.20 all series tested at room temperature at an extension rate of 1.00 mm/min have been plotted as a single series. Again, it is possible to identify two distinct families: one formed by the pipe (unjointed) and soldered (alloy 12 and 23) samples, and the other by the brazed samples (CP 203). The first of these families lies between ln σ = 6.0 and ln σ = 6.2, the long tail on this grouping showing that the majority of variation arises from the series assessing practitioner variability (as marked by green dashes), where we see a spread over a large region of the x-axis and in fact spreading into the second family of series. This can be compared with the second family, lying between ln σ = 5.7 and ln σ = 6.0, where the tail is spread over a larger range of both the x and y axes, and furthermore is made up of outliers from several series rather than just one.

In Figure 5.21 Weibull series for alloy 12 soldered joints have been plotted including both coupler based soldered joints and swaged soldered joints. The swaged joint characteristics are similar to the equivalent coupler jointed series. The impact of testing at elevated temperature on the Weibull series can also be observed. The elevated temperature resulting in a clear reduction of both the Weibull modulus and characteristic strength. The greatest reduction is observed for testing conducted at 50 °C in the hydrogen charging test environment.

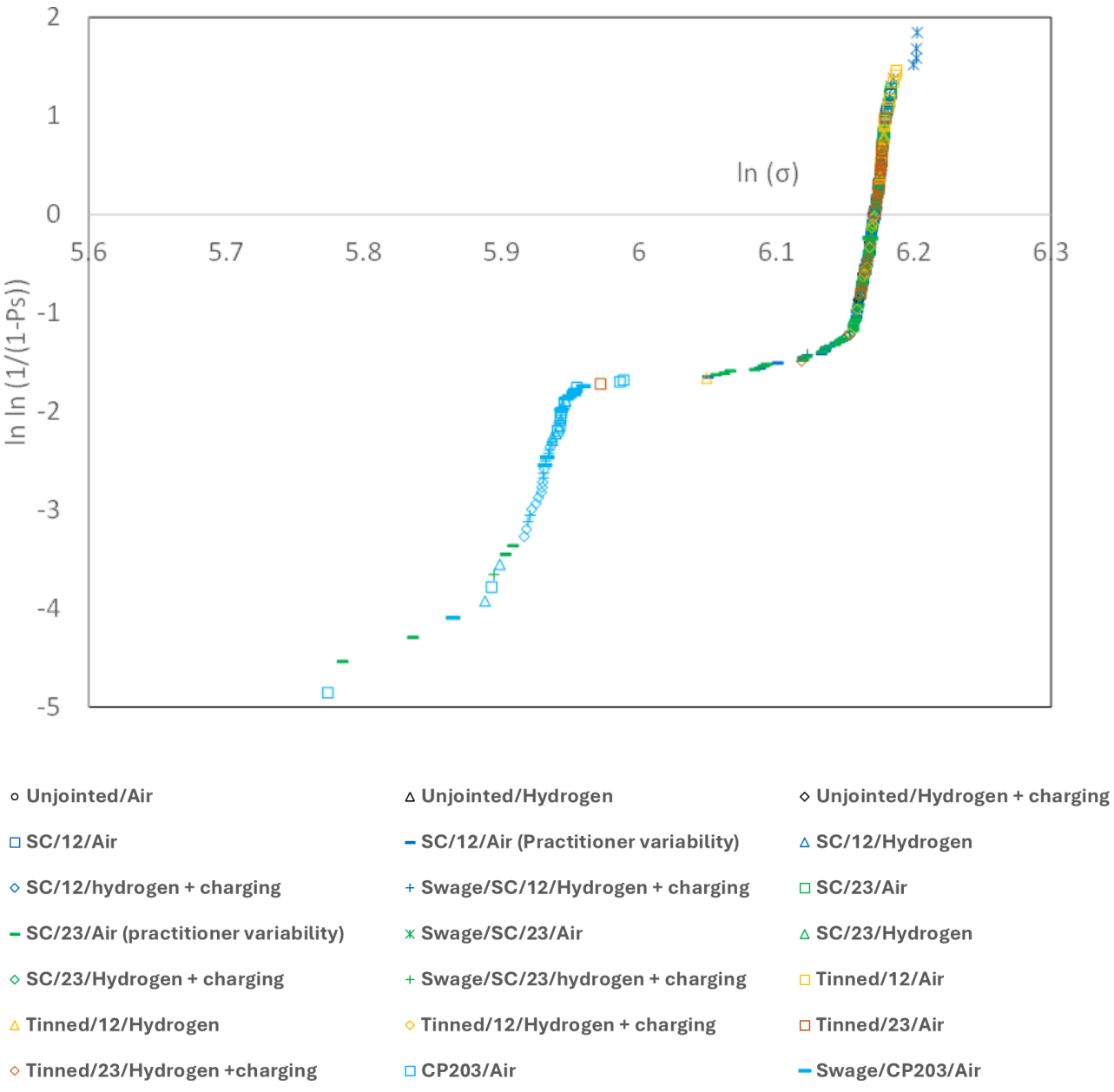

Figure 5.20 - All data for samples tested at room temperature treated as a single series for Weibull analysis.

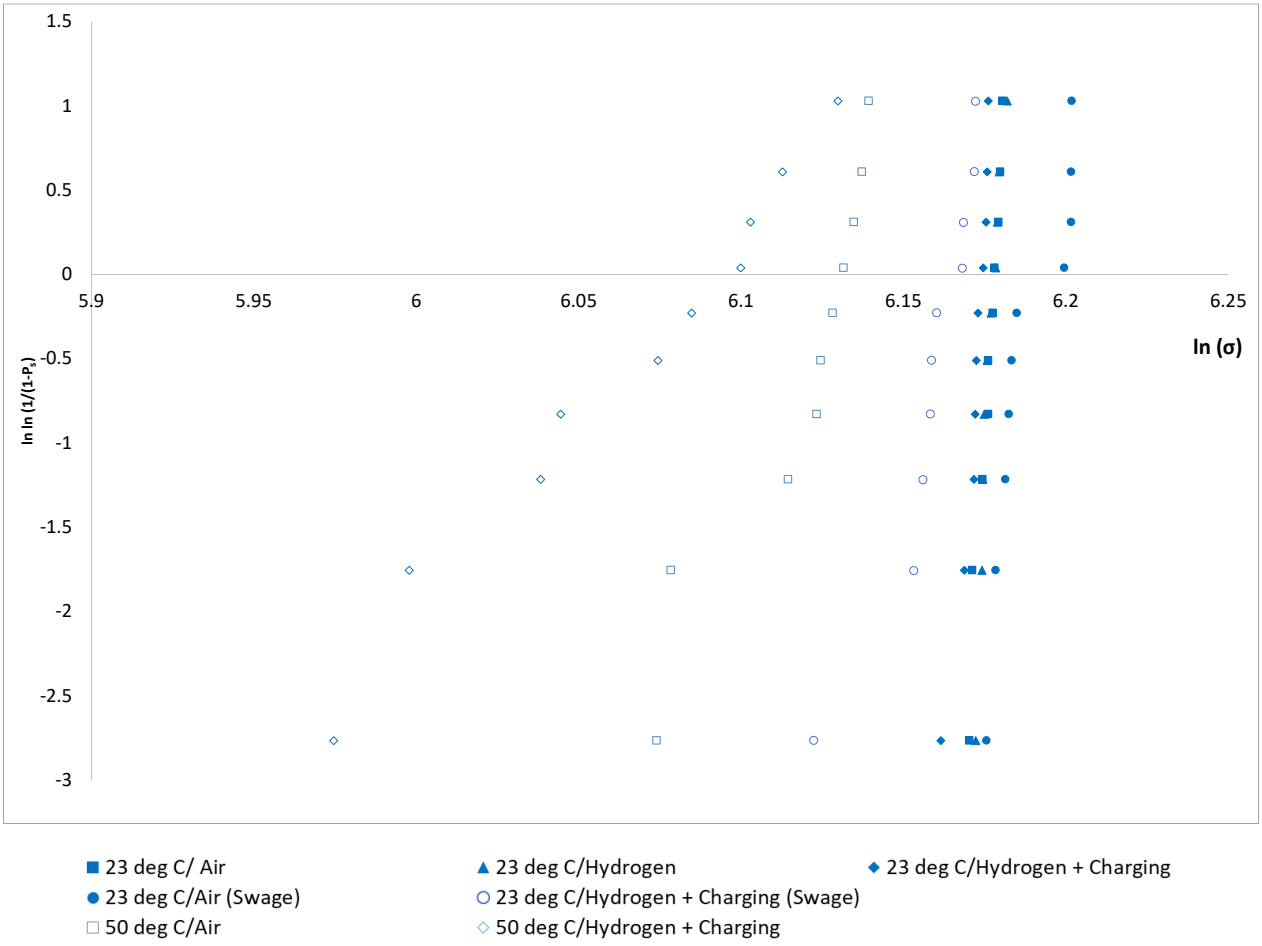

Figure 5.21 – Comparison of performance under various environmental conditions (temperature, atmosphere, charging), for the combination of alloy 12 solder with self-cleaning flux, and comparing coupling and swage type fittings.

5.13 Combined inter series analysis

5.13.1 UTS

As displayed in Figure 5.22, the testing in gaseous hydrogen results in little change to the mean UTS relative to equivalent baseline results in air. Hydrogen charging results in a decrease in mean UTS relative to the baseline testing in air. This is the case for both testing at both temperatures (room temperature and 50 °C), although the decrease in UTS at the elevated temperature is greater. This is true for all series tested at an extension rate of 1.00 mm/min with the exceptions of alloy 23 tinned flux (series 2I and 2J). This is because of an abnormally low result in the baseline series 1H reduced the average, highlighted in Figure 5.9, this occurred due to poor joint quality with solder failing to fully infiltrate the joint. Should this result be excluded from the mean UTS would also decrease for the alloy 23 tinned flux specimens and would be in line with the other soldered joint series.

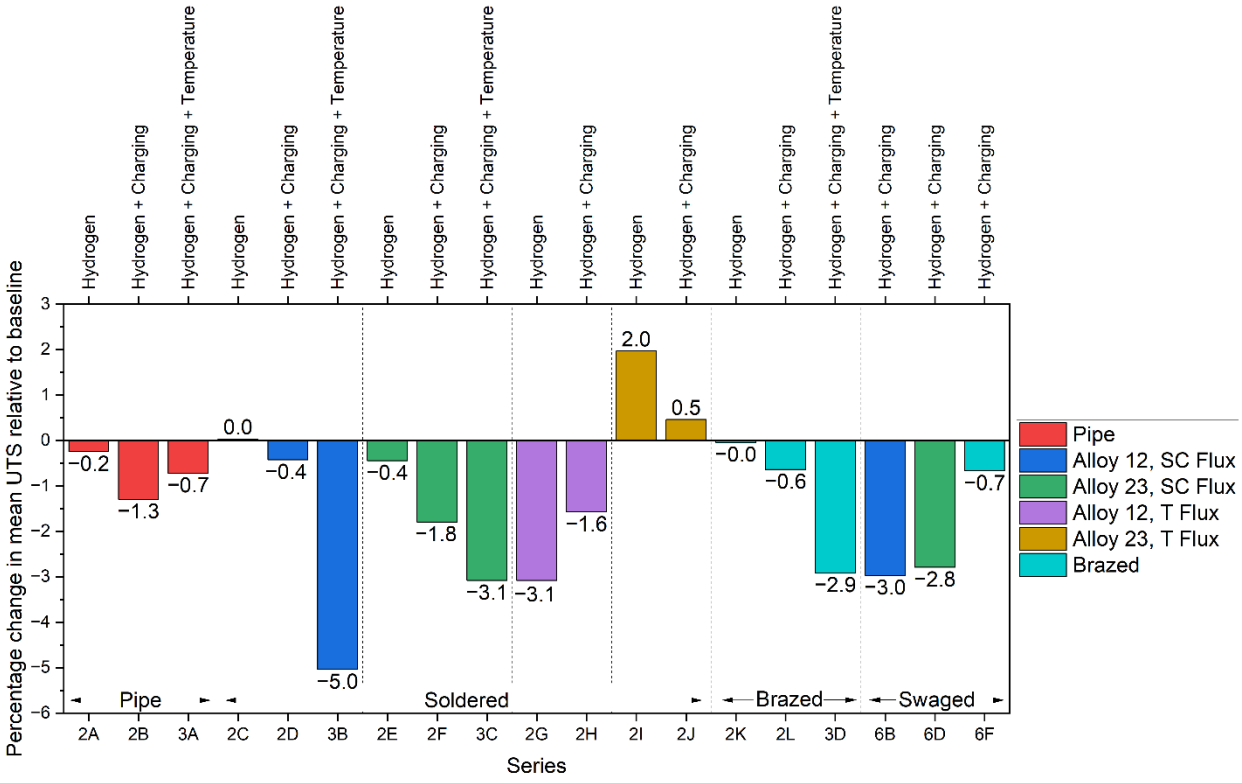

Figure 5.22 – The percentage change in the mean UTS relative to the according baseline series for all series tested at an extension rate of 1.00 mm/min. Series have been grouped depending on the joint type into pipe, soldered, brazed, and swaged samples as labelled at the bottom of the plot. All tests conducted at room temperature, with the exception of those noted by "temperature" which were conducted at ~50°C.

5.13.2 Strain to Failure

There is no consistent trend in the change in mean strain to failure for either hydrogen or hydrogen charging at room temperature (Figure 5.23). Some series exhibited an increase, others a decrease. This variation is believed to be because of the change in failure mode frequency between series. Whilst hydrogen or hydrogen charging did not have a consistent impact on failure mode, the variation in failure mode distribution within each series has a significant impact on mean strain, with the jointed failures typically occurring at lower strains than pipe failures. Isolating the jointed failures and calculating series averages using jointed failure data only as a point of comparison between each series did not offer any clear insight, the number of jointed failures per series was too low for a meaningful analysis using this data only, mean values were sensitive to any abnormally low values.

Hydrogen charging at elevated temperature resulted in a relative decrease in mean strain for pipe and soldered samples, however, not for brazed samples. Testing at elevated temperature resulted in failure only occurring at the joint, allowing the mean calculation relative to baseline to be made over a full series of ten samples. As a result, this decrease in mean strain at failure for jointed samples is believed to be the best measure of the impact of hydrogen charging on of soldered joint mechanical capacity. Hydrogen charging at elevated temperature resulted in a decrease in mean strain at failure for all soldered samples tested, as well as the pipe samples. No significant change in mean strain at failure was observed for brazed samples. Hydrogen charging for the majority of pipe and soldered samples consistently resulted in an increase in the series variability of strain at failure values relative to the equivalent baseline series in air; again, no notable trend was observed for brazed samples.

In Figure 5.23 there are a number of series with an increase in strain at failure in either or both the hydrogen and hydrogen charging test environments. Notably series 2E and 2I with a 30.0% and 46.8% increase in mean strain at failure relative to their respective baseline series. For both of these series this is attributed to a lower occurrence of jointed failure in the hydrogen test environment, with two jointed failures present in the 2E series and just one jointed failure present in the 2I series. Neither gaseous nor charged hydrogen is believed to impact the failure mode and there is no clear trend between series. Jointed failures of soldered samples typically occur at lower strains than pipe based failures resulting in the measured mean increase. Isolating the jointed failure and calculating the same averages is not believed to be appropriate as the sample size becomes too small for the mean to have much value.

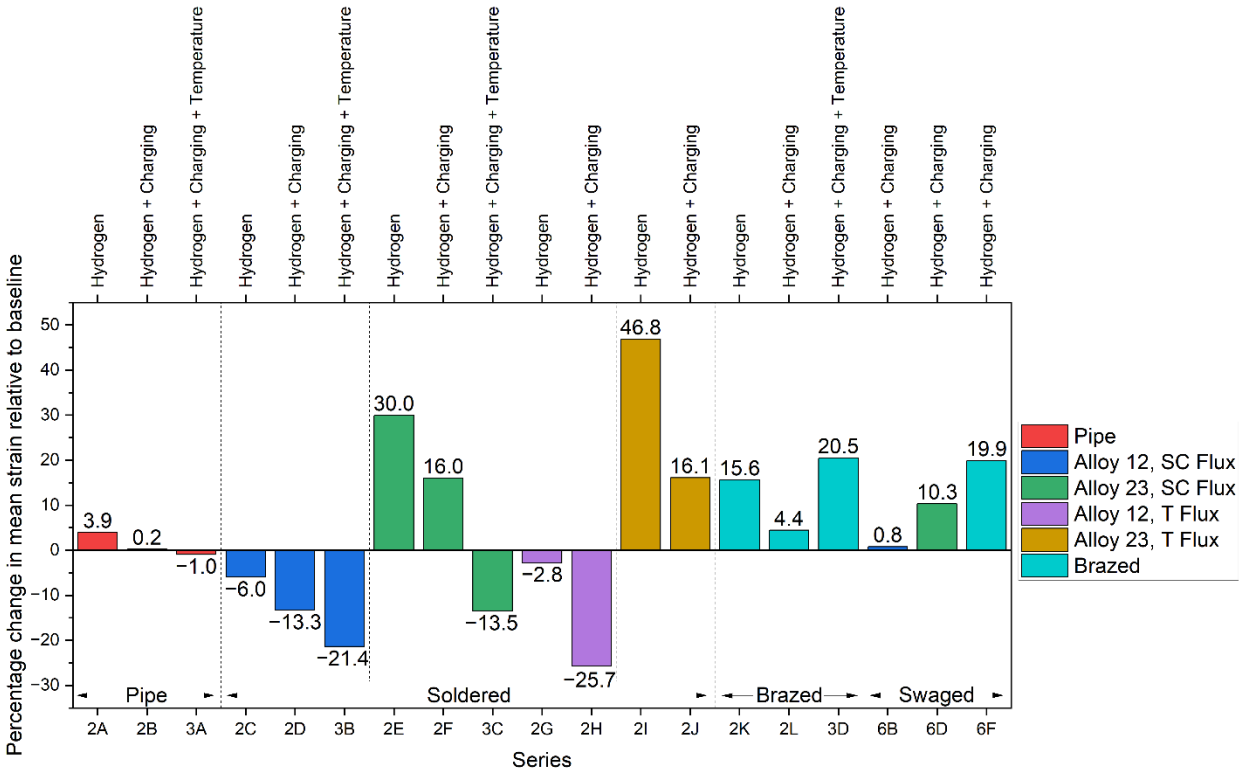

Figure 5.23 – The percentage change in the mean strain to failure relative to the baseline for all series tested, at an extension rate of 1.00 mm/min. Series have been grouped depending on the joint type into pipe, soldered, brazed, and swaged samples. All tests conducted at room temperature, with the exception of those noted by “temperature” which were conducted at ~50°C.

6 Concluding Remarks

6.1 Summary

The purpose of this project was to research and provide evidence of the suitability of solder and brazing alloys for use in low pressure hydrogen gas installations. These alloys are used to make joints in copper pipework and the suitability of these joints has been assessed through tensile testing in different environments at extension rates of 1.00, 0.10 and 0.01 mm/min. The results of this testing and statistical analysis of the test data underpin this assessment.

In total, 456 tensile tests of copper pipe specimens have been completed. Samples were flat gripped at each for tensile testing. Each unique test condition and specimen material combination was conducted ten times at an extension rate of 1.00 mm/min, and three times for the slower extension rates of 0.10 and 0.01 mm/min. The majority of specimens tested contained a joint made using a solder and flux or brazed using a braze filler. A leaded and an unleaded solder have been tested in combination with a self-cleaning or tinned flux; brazed joints were made with a copper phosphorus braze filler. Joints were formed using a coupler fitting or by swaging the pipe to create a socket type joint.

The impact of hydrogen has been assessed through testing series of specimens in different environments: air (to provide a baseline), hydrogen, and hydrogen charging. Testing has also been conducted at two temperatures: room temperature (~23 °C) and at a target temperature of 50 °C. Testing in gaseous hydrogen was achieved by filling the specimen with 1 bar gaseous hydrogen and crimping each end flat to seal the hydrogen within the hollow sample. The hydrogen charging test environment was achieved through immersion charging, specifically immersing the samples in a 20% ammonium thiocyanate solution at 50 °C for 72 hours. The purpose of this charging is to absorb hydrogen into the sample, attempting to emulate an absorbed hydrogen content the specimen may experience after 50 years of service for up to 250 mbar hydrogen. Following charging the specimens were also filled with 1 bar hydrogen and crimped flat at each end. It was intended to test the sample in a more extreme hydrogen environment than it would experience in service, and this was achieved by the higher hydrogen gas pressure and a higher induced level of absorbed hydrogen (although it should be noted this has not been experimentally validated).

The UTS and strain at failure was calculated for each specimen from the force displacement data, and it was these characteristic data points that formed the basis of the analysis. The strain to failure was defined as the point at which a 10% drop occurs from the UTS. This analysis was supported by a Weibull analysis based on the UTS conducted for all series of ten specimens.

6.2 Key Findings

The key findings of the work are as follows:

- Relative to testing in air, testing in gaseous hydrogen at an extension rate of 1.00 mm/min has no significant impact on joint mechanical capacity. There is a slight reduction in UTS (less than 5%) for specimens tested at 0.10 mm/min and 0.01 mm/min extension rates. Extension rates of 1.00, 0.10 and 0.01 mm/min correspond to average strain rates of 1.4×10^{-4}, 1.4×10^{-5} and 1.5×10^{-6} s^{-1} respectively.
- Absorbed hydrogen by hydrogen charging appears to have an effect on joint mechanical capacity, reducing the UTS of all specimens by up to 5%, relative to baseline testing in air. The strain at failure for soldered samples has been observed to decrease by up to 21%, relative to baseline testing in air. The variability of the strain at failure for soldered samples increased for hydrogen charged samples, compared to those tested in air. There is no clear effect of absorbed hydrogen on the strain to failure for pipe or brazed samples.
- Hydrogen, whether gaseous or absorbed through hydrogen charging, has no clear impact on joint failure mode.

- For all environments tested (air, hydrogen and hydrogen charging at two temperatures) the tensile behaviour of soldered specimens is dominated by the base pipe material and is insensitive to the solder, flux, or joint type.
- The premature failure of soldered joints occurs where solder fails to fully infiltrate the joint. This is applicable to all test cases and joint material combinations.
- The tensile response of brazed joints differs to soldered joints, with brazed joints reaching on average, a 20% lower UTS, but failing at up to twice the strain.
- Testing at an elevated temperature of 50 °C has no significant effect on brazed joints. For soldered joints, testing at temperature results in failure only at the joint.

6.3 Further Work

6.3.1 Slow Strain Rate Testing

As discussed in Section 5.12.1, the soldered samples at lower extension rates failed at progressively lower strains. As a result, it is possible the test duration was not long enough to allow hydrogen absorption into the specimen and resulting embrittlement. To facilitate hydrogen absorption specimens charged with gaseous hydrogen prior to testing and/or slower extension rates could be explored for soldered samples.

The time critical nature of the slow strain rate tests added following the interim amendment to the test plan limited the number of tests achievable to three for each test series. Conducting more slow strain rate tests would facilitate an improved statistical analysis.

6.3.2 Fatigue Testing

Tensile testing has been established to determine fundamental mechanical properties/material behaviour and interaction with environment – it's not explicitly meant to simulate the loading condition. The loads applied to the specimens during tensile testing are far higher than copper pipework should see in service. Total life fatigue testing would allow the number of cycles to failure of specimens to be assessed at subcritical loads, less than the UTS, which may be more representative of the loads the pipe will experience in service. High cycle fatigue testing is a common test method used to assess hydrogen compatibility as the extended test duration and dynamic load facilitates hydrogen absorption from the gaseous phase into the sample.

6.3.3 Hydrogen Charging Efficacy

Whilst we anticipate the immersion charging regime used has resulted in an absorbed level of hydrogen greater than the specimen would see in service, it is desirable to quantify this experimentally. Assessing this would grant insight into what gaseous conditions the absorbed hydrogen from ammonium thiocyanate immersion charging is equivalent to. This analysis was not possible within the timeline of this project, but, is seen as valuable as a direct measure of the equivalency of the data obtained with real world conditions.

References

[1] Institution of Gas Engineers & Managers (IGEM), “IGEM/H/1 - Reference Standard for low pressure hydrogen utilisation,” IGEM, 2023.

[2] Department for Energy Security and Net Zero, “Invitation to Tender: Research into Suitability of Solder and Brazing Alloys for Use in Low Pressure Hydrogen Gas Installations,” London, 2023.

[3] Frazer-Nash Consultancy, “Research into Suitability of Solder and Brazing Alloys for Use in Low Pressure Hydrogen Gas Installations: Test Plan,” 2023.

[4] Frazer-Nash Consultancy, “Interim Report: Research into Suitability of Solder and Brazing Alloys for Use in Low Pressure Hydrogen Gas Installtions,” 2024.

[5] M. Ichiba, K. Takai and J. Sakai, “Effects of Test Conditions on Corrosion Reactions and Hydrogen Absorption in Hydrogen Embrittlement Tests Using an Ammonium Thiocyanate Solution,” *ISIJ International,* pp. 397-404, 2016.

[6] ASTM International, “ASTM G142-98(2022): Standard Test Method for Determination of Susceptibility of Metals to Embrittlement in Hydrogen Containing Environments at High Pressure, High Temperature, or Both,” 2022.

[7] A. Drexler, F. Konert, O. Sobol, M. Rhode, J. Domitner, C. Sommitsch and T. Bollinghaus, “Enhanced gaseous hydrogen solubility in ferritic and martensitic steels at low temperatures,” *International Journal of Hydrogen Energy,* p. 15, 2022.

[8] H. Horinouchi, M. Shinohara, Otsuka, T., K. Hashizume and T. Tanabe, “Determination of hydrogen diffusion and permeation coefficients in pure copper at near room temperature by means of tritium tracer techniques,” *Journal of Alloys and Compounds,* vol. 580, pp. S73-S75, 2013.

[9] K. F. Hans Magnusson, “Diffusion, Permeation and Solubility of Hydrogen in Copper,” *Journal of Phase Equilibria and Diffusion,* vol. 38, pp. 65-69, 2017.

[10] D. Parker, T. Legg and C. Folland, “A new daily Central England temperature series,” *International Journal of Climatology,* vol. 12, pp. 317-342, 1992.

[11] D. Guade-Fugarolas, “Description of hydrogen transport through a metal wall, and prediction of embrittlement risk,” dgaude Prime Innovation SLU, Vilassar de Mar, 2019.

[12] K.-i. Ebihara, T. Iwamoto, Y. Matsubara, H. Yamada, T. Okamura, W. Urushihara and T. Omura, “Numerical Analysis of Influence of Hydrogen Charing Metod on Thermal Desorption Spectra for Pre-strained High-Strength Steel,” *ISIJ International,* vol. 54, pp. 153-159, 2014.

[13] M. Truschner, A. Trautmann and G. Mori, “The Basics of Hydrogen Uptake in Iron and Steel,” *Berg Huettenmaenn Monatsh,* vol. 166, pp. 443-449, 201.

[14] P. Klemarczyk and J. Guthrie, Advance in Structural Ahesive Bonding, Chapter 5 - Advances in anaerobic and cyanoacrylate adhesives, Woodhead Publishing, 2010.

A.1 Hydrogen Charging Methodology

For reference, the Annex from the test plan [1] is included here. A process of accelerated hydrogen uptake can be achieved in the laboratory; this is referred to as charging.

Charging the samples involves adsorption of hydrogen into the material, typically at an accelerated rate. By charging the samples with a representative concentration of hydrogen to what may be experienced under normal operating conditions, the effects of adsorbed hydrogen, hydrogen present within the material's crystal structure, can be assessed.

In terms of how much 'charging' is necessary, how this will be affected, and how this might be verified, it is necessary to consider the normal lifetime operating conditions experienced by the material or component (in this case, as specified in the Invitation to Tender (ITT) documentation). In addressing the first of these points, the expected saturation concentration and rate of diffusion of hydrogen into copper has been calculated. The solubility model used to assess the theoretical hydrogen uptake is an extension of Sievert's Law to gases at low temperatures proposed, parametrised, and validated by Drexler et al. [7]:

$$c_H = K_0(T)\sqrt{f}\exp\left(-\frac{\Delta H_S - \sigma_H V_H}{RT}\right), molm^{-3}MPa^{0.5} \quad (1)$$

The permeation rate through the pipe wall has been calculated using two experimentally derived permeation models:

- Permeation model 1 [8]:

$$P = (2.8 \pm 0.4) \times 10^{-6}\exp\left(\frac{-85 \pm 2\left(\frac{kJ}{mol}\right)}{RT}\right), molm^{-1}s^{-1}Pa^{-\frac{1}{2}} \quad (2)$$

- Permeation model 2 [9]:

$$P_{H,Cu}^{FCC} = 4.5 \pm 10^{-4}\exp\left(-\frac{84320}{RT}\right), molm^{-1}s^{-1}atm^{-0.5} \quad (3)$$

The permeation rate and solubility have been calculated for a copper pipe with an outer diameter of 22 mm and wall thickness 0.9 mm for the following operating conditions:

- 100% hydrogen (nominal).
- 250 mbar.
- Historic Central England monthly mean air temperature for the last 50 years from May 2023 [10].

To calculate the length of time, under the defined operating conditions, required to reach the saturation concentration of hydrogen in the copper pipe, Equation (1), it has been assumed all adsorbed hydrogen first saturates the trapping sites in the copper pipe. This trapping behaviour, before reaching steady state adsorption-desorption of hydrogen in copper is reported by Horinouchi et al [8] and Guade-Fugarolas et al [11]. Once hydrogen trapping sites have been saturated, steady-state permeation through the copper pipe wall will result in the theoretic hydrogen uptake concentration Equation (1). Figure A.1 depicts the overlap between solubility concentration and cumulative hydrogen permeation used to calculate the time to saturation for one metre of copper pipe in the defined conditions.

Evident in Figure A.1 is that the copper pipe will hit saturation under the defined conditions with the assumptions made, the copper pipe will be likely be operating at its hydrogen saturation concentration, Equation (1), for the majority of its operating lifetime. The time to reach saturation has been calculated using the mean average hydrogen solubility over the past 50 years, and a hydrogen concentration of 3.84 x 10^{-5} mol·m^{-3} or 0.27 ppb. This indicates that the time to reach saturation for Permeation Model 1 is 10.2 years and 15.1 years for Model 2.

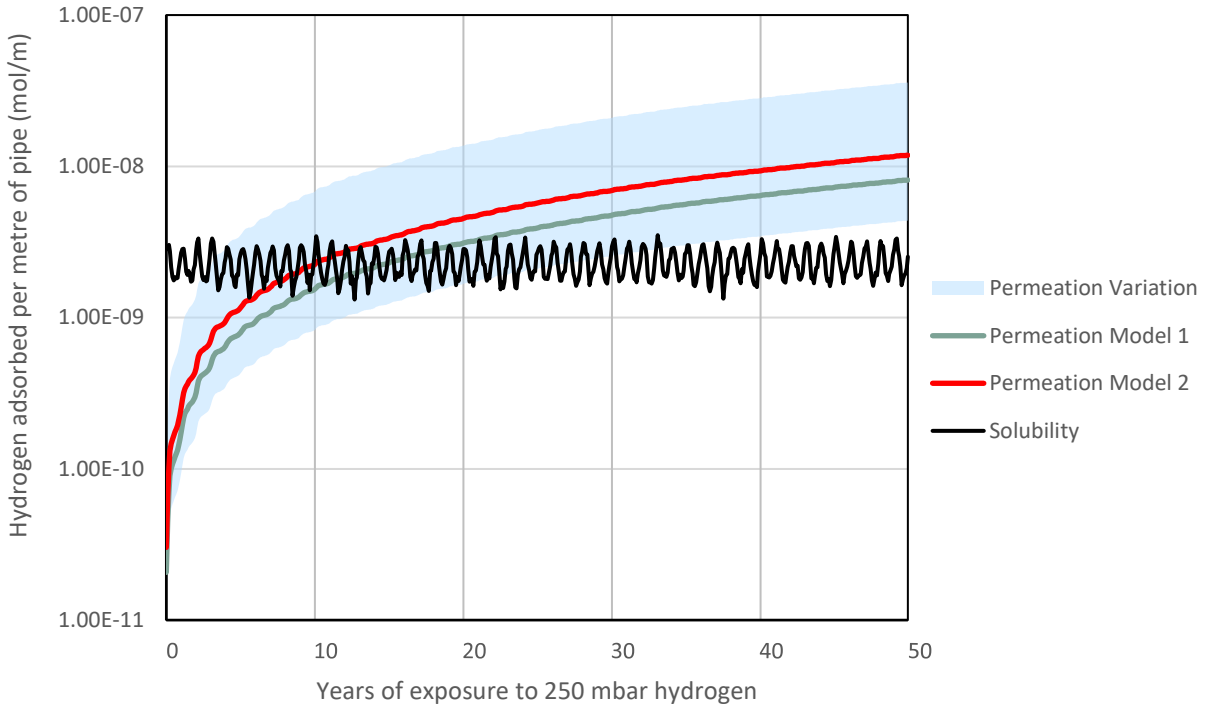

Figure A.1 – Solubility concentration, Equation (1), and cumulative hydrogen permeation using Permeation Model 1, Equation (2), and Permeation 2, Equation (3), per metre of pipe, calculated using the last 50 years of mean monthly Central England temperature. The Permeation Variation is calculated using the upper and lower bounds of Permeation Model 1, Equation (2).

Modelling the same scenario using a constant temperature of 18°C yields a time to reach saturation of 6.0 years for Permeation Model 1 and 8.7 years for Permeation Model 2. As the permeation rate of hydrogen in copper is more temperature dependent than its solubility, increasing the temperature will decrease the time to reach saturation. The scenario and assumptions behind Figure A.1 are pessimistic, pipes in a warmer environment such as domestic plumbing will reach hydrogen saturation earlier. Global warming will also act to decrease the time to reach saturation, although the specific impact of this is harder to model, given the climatic nature of this effect, and localised variability. For example, large urban conurbations tend to be warmer overall, compared with more rural settings.

A wider debate in the materials community is whether the activation energy required for dissociative chemisorption of hydrogen into the host metallic material is ever present. Modelling this activated process through various Arrhenius relationships, as shown above, suggests that dissociative chemisorption will occur within the defined operating conditions, albeit at very slow rates. Figure A.1 and the calculated time to saturation for the copper pipe, demonstrates this and thus the need for sample charging. To fully assess the hydrogen compatibility of the materials in question, as part of the test plan, samples will be loaded with a representative amount of hydrogen, so that as part of this work, the impact of hydrogen embrittlement on the mechanical properties can be quantified.

Whilst the solubility and permeability for copper can be estimated using equations and values published in literature, as demonstrated, the same process cannot be meaningfully replicated for the solder and brazing material in question

due to a lack of published research. However, it is expected that the solubility and permeation rate for solder and brazing material will be higher than that of copper. Hydrogen charging a material can be carried out through four different methods:

- Gaseous charging, using an elevated pressure and/or temperature to increase the rate of hydrogen absorption into the material.
- Electrochemical charging, immersing the sample in an electrolyte solution and applying a potential difference to promote hydrogen adsorption.
- Immersion charging, immersing the sample in an acidic solution which will enhance the dissociation and adsorption of hydrogen into the material.
- Cathodic charging, promoting hydrogen adsorption by using the sample as a cathode in an electrochemical cell.

Hydrogen charging is analogous to accelerated aging: it is essential to undertake a process which genuinely mimics the impact of the desired period of operation to be assessed, without introducing spurious artefacts that would not be seen in real life. Relative to other hydrogen charging methods, immersion charging has shown to result in adsorbed hydrogen concentrations that are most representative of the expected uptake under the operating definitions defined in the ITT. This process was selected for the following reasons:

- Immersion charging at open circuit potential has been shown to result in lower hydrogen concentration in the material. Given the low temperatures and pressures and resulting low theoretic uptake of hydrogen into the material, this is desirable.
- Immersion charging is a less aggressive way to promote hydrogen adsorption than electrochemical or cathodic charging, which create a more corrosive environment. This can damage the sample as well as typically resulting in a higher hydrogen concentration absorbed into the material.
- Conducting gaseous charging at high elevated pressures and/or temperatures may lead to sample damage, particularly at the joint, which is likely to be more temperature sensitive than the copper. Gaseous charging at temperatures and pressures closer to the operating conditions will take a long time.
- Immersion charging is easy to conduct, consistent, and quick, with a typical loading period of 2-4 days.

As part of Stage 1 of the project further research will be conducted into an appropriate immersion charging regime that will load the samples with a representative hydrogen concentration whilst limiting sample damage. Example immersion regimes taken from literature for other metallic compatibility testing include:

- Immersion in 20% NH_4SCN solution for 48 hours [12].
- Immersion in 3.5% NaCl between 2 and 336 hours [13].
- Immersion in 1 mol H_2SO_4 between 2 and 336 hours [13].

A.2 Weibull analysis data

Table A.2 – Summary of Weibull behaviour for all final series tests at an extension rate of 1.00 mm/min.

Series	Characteristic strength, σ_0	Weibull modulus, m	R^2
1A	480	187	0.8867
1B	462	133	0.9576
1C	482	324	0.9671
1D	454	46	0.9641
1E	483	393	0.7572
1F	464	35	0.8706
1G	485	263	0.8659
1H	481	147	0.7025
1I	389	17	0.8159
1J	368	83	0.9387
2A	478	254	0.9053
2B	473	311	0.9566
2C	482	373	0.9267
2D	480	252	0.9098
2E	481	381	0.9626
2F	475	166	0.7441
2G	481	632	0.9313
2H	477	196	0.9661
2I	481	693	0.8715
2J	476	379	0.9525
2K	381	212	0.9663
2L	376	193	0.9682
3A	457	388	0.9787
3B	441	22	0.9774
3C	453	25	0.9231
3D	358	60	0.9691
5A-P1	475	35	0.8422
5A-P2	478	26	0.8319
5A-P3	479	259	0.9372
5A-P4	474	50	0.7457

Series	Characteristic strength, σ_0	Weibull modulus, m	R^2
5A-P5	478	239	0.9803
5B-P1	411	8	0.9194
5B-P2	465	63	0.9308
5B-P3	474	357	0.8094
5B-P4	477	531	0.9013
5B-P5	479	471	0.7188
5A	474	35	0.7407
5B	866	9	0.7252
6A	490	96	0.8072
6B	476	74	0.8678
6C	480	202	0.9623
6D	477	195	0.9557
6E	384	92	0.941
6F	379	142	0.9431

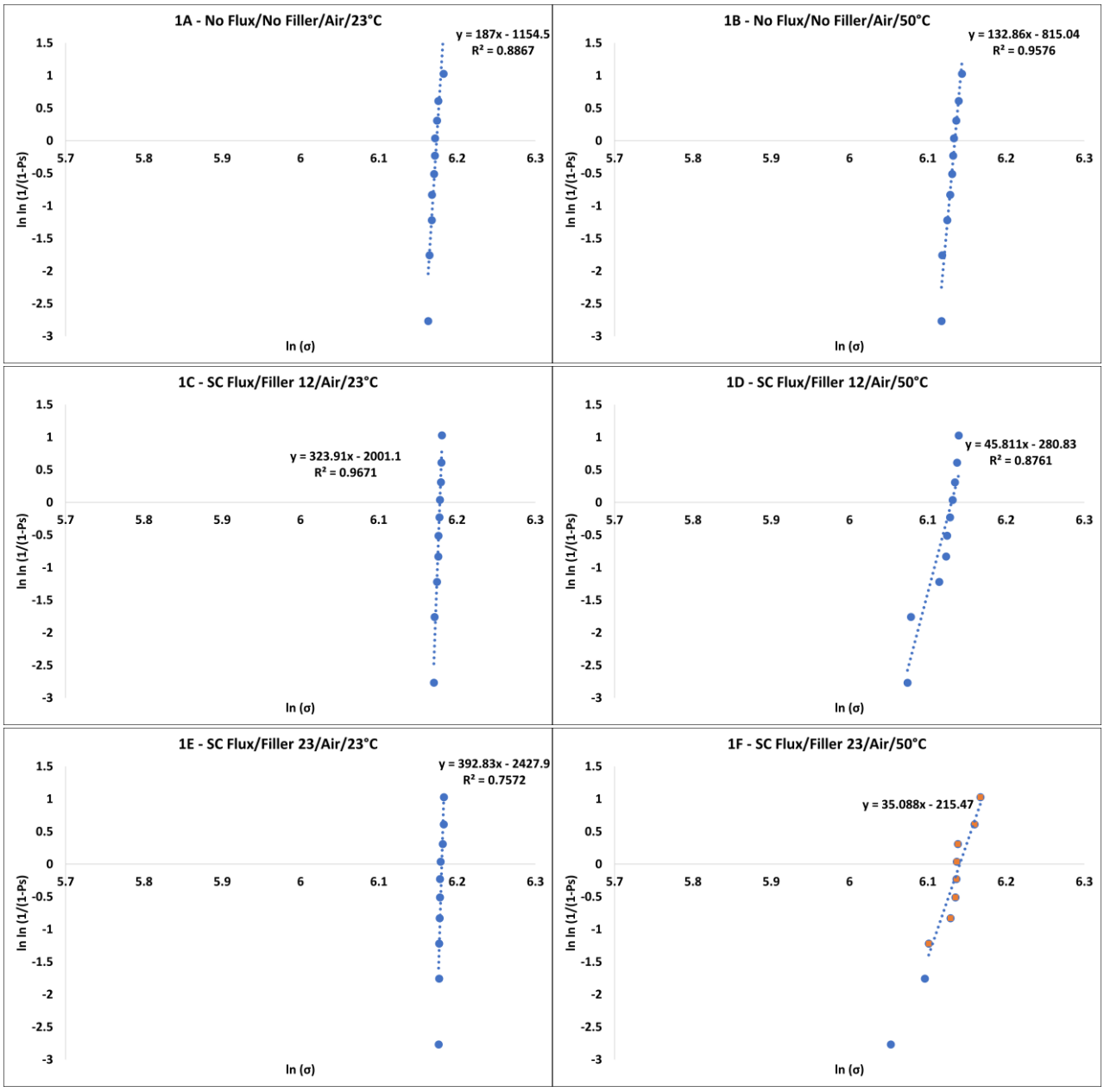

Figure A.2 – Individual series from Figure 5.19, for reference

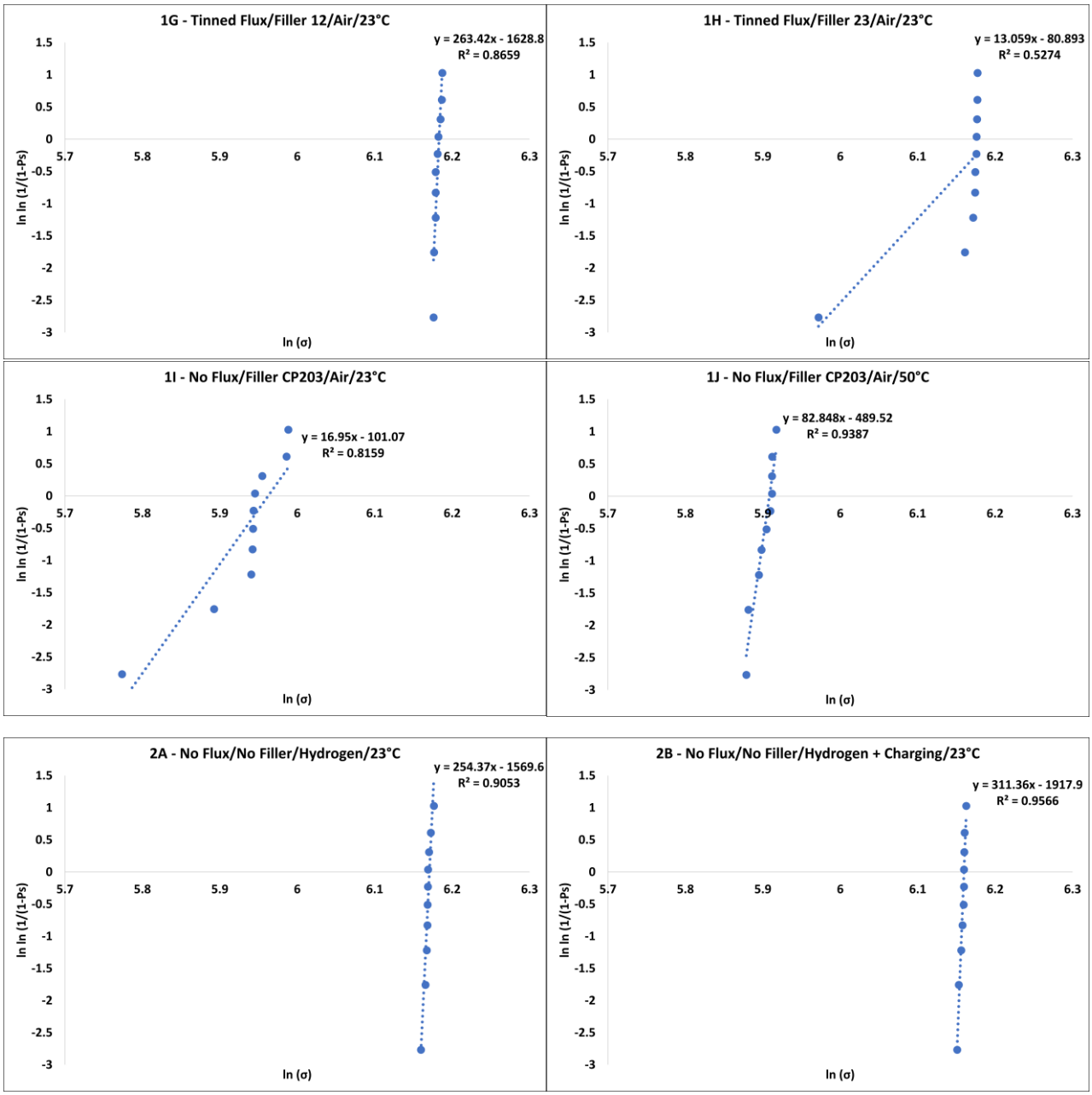

Figure A.2 (continued) – Individual series from Figure 5.19, for reference

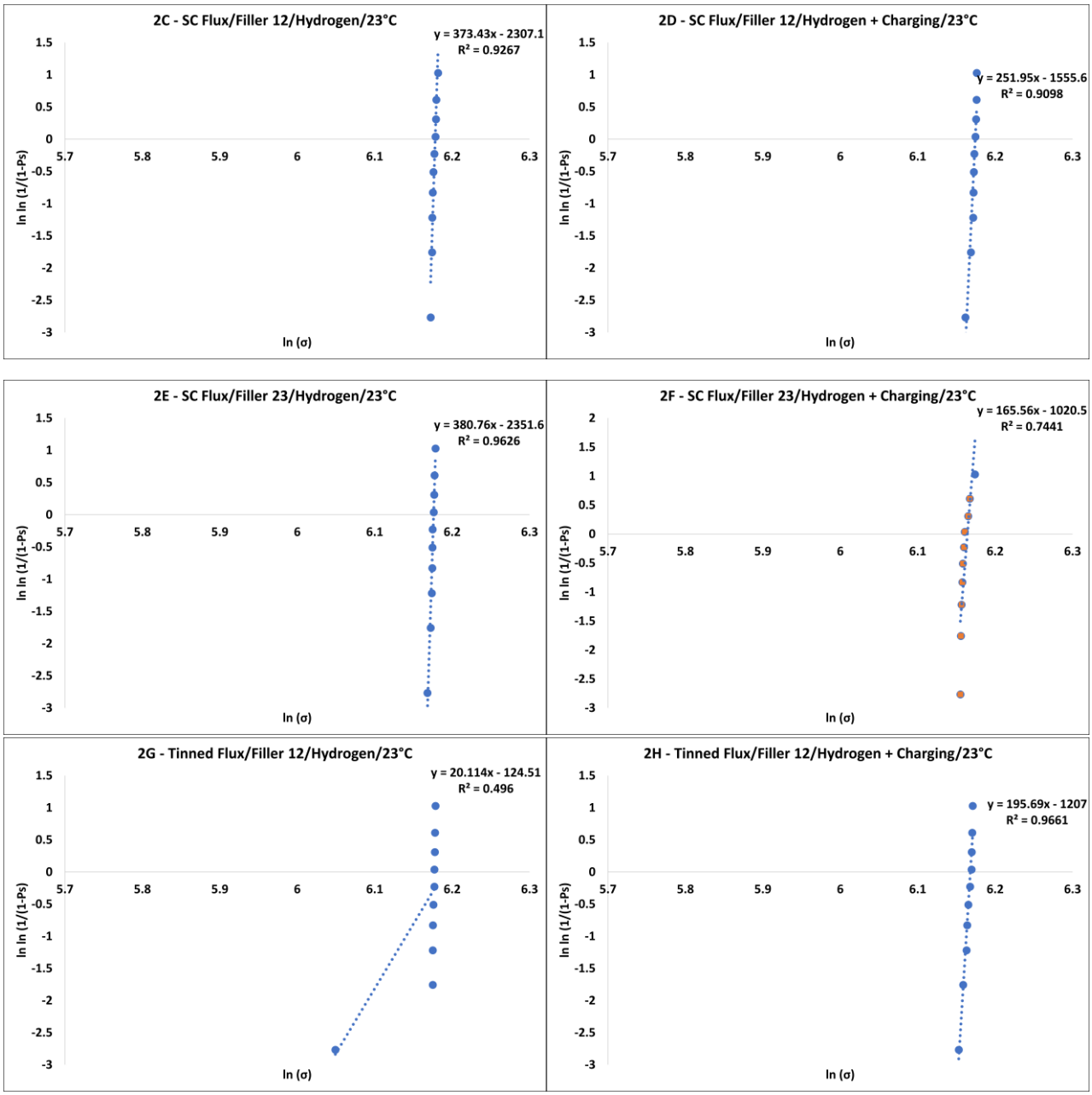

Figure A.2 (continued) – Individual series from Figure 5.19, for reference

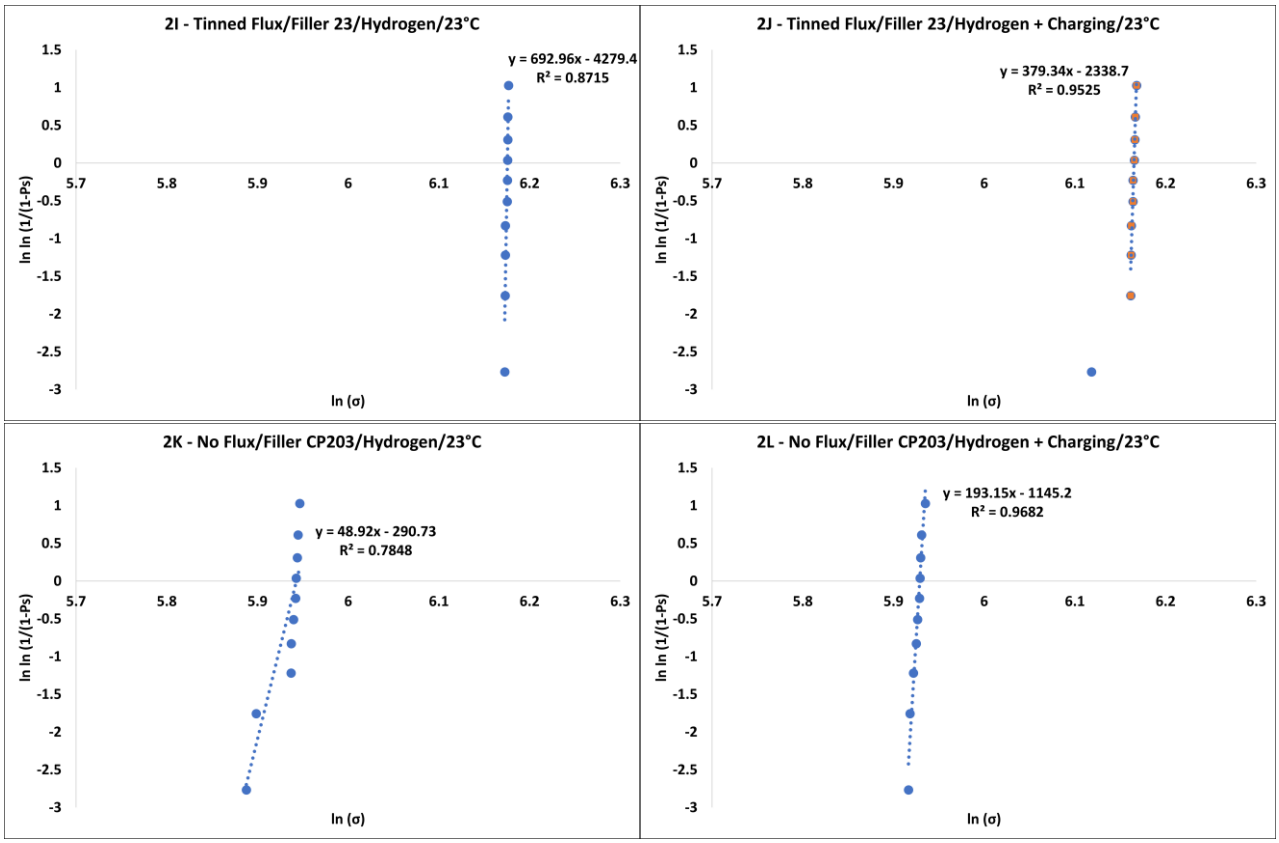

Figure A.2 (continued) – Individual series from Figure 5.19, for reference

Hill Park South
KBR Campus
Springfield Drive
Leatherhead
Surrey
KT22 7LH

Tel: +44 (0)1306 885050

fnc.co.uk

Offices at:
Bristol, Burton-on-Trent, Dorchester, Glasgow, Gloucester,
Harwell, Leatherhead, Manchester, Middlesbrough,
Plymouth and Portsmouth